Silurian K-bentonites of the Welsh Borderlands: Geochemistry, mineralogy and K-Ar ages of illitization

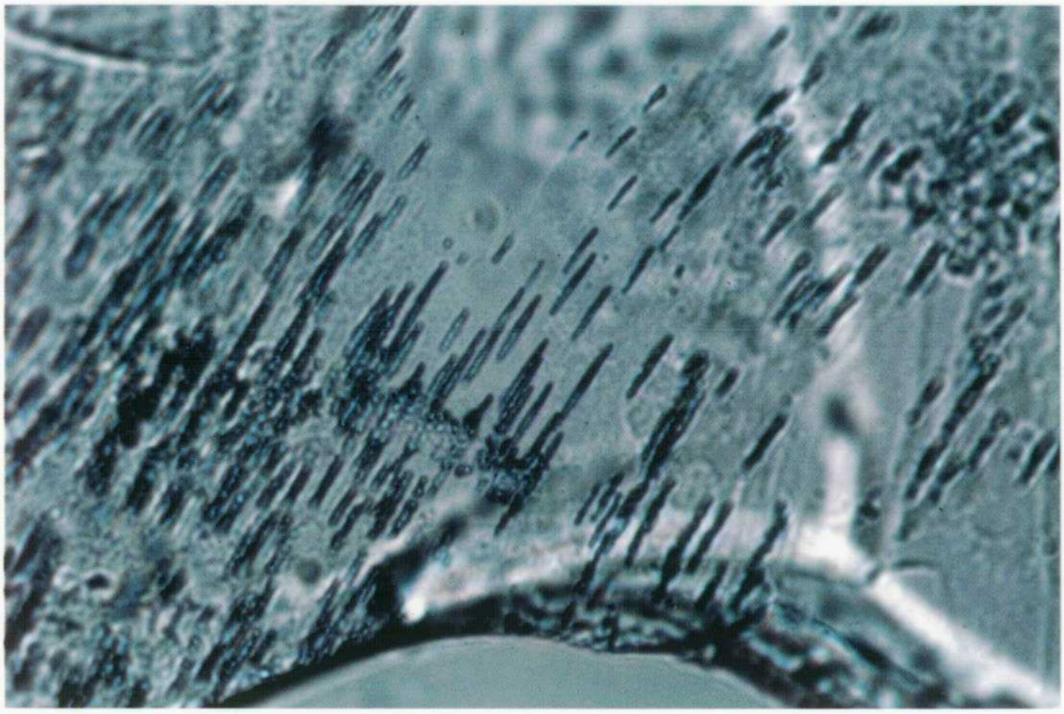

British Geological Survey

BRITISH GEOLOGICAL SURVEY

TECHNICAL REPORT WG/96/45

Mineralogy & Petrology Series

Silurian K-bentonites of the Welsh Borderlands: Geochemistry, mineralogy and K-Ar ages of illitization

W D Huff[1], D J Morgan and C C Rundle[2]

[1] Department of Geology, University of Cincinnati, Cincinnati, Ohio 45221-0013, USA

[2] NERC Isotope Geosciences Laboratory, Keyworth, Nottingham NG12 5GG

Cover illustration
Linear surface features on quartz phenocryst from K-bentonite

Bibliographic reference
Huff, W D, Morgan, D J and Rundle, C C. 1996. Silurian K-bentonites of the Welsh Borderlands: Geochemistry, mineralogy and K-Ar ages of illitization. *British Geological Survey Technical Report WG/96/45*

Keyworth, Nottingham
British Geological Survey 1996

Abstract: More than 100 K-bentonite beds occurring in Llandovery through Ludlow strata of the Welsh Borderlands are described. K-bentonite sequences are preserved in the deep water Llandovery Purple Shales, the off-lap facies of the Wenlock Series, turbiditic facies of the Welsh Basin, slope facies of the early Ludlow Eltonian Beds and carbonate platform deposits of mid-Ludlow to late-Ludlow Bringewoodian Beds. Individual beds range from 2 cm to 1 m in thickness and typically consist of white to greenish-grey plastic clay with minor amounts of mainly volcanogenic, non-clay minerals. The <2 μm fractions of the K-bentonites consist of random to regularly interstratified (R0-R3) illite/smectite with lesser amounts of discrete illite, chlorite and kaolinite. Non-clay minerals include a volcanic suite of quartz, biotite, apatite, zircon and albite-oligoclase. K-Ar ages of illite in the I/S are positively correlated with %I, indicating evidence of a slow and continuous process of illitization from the Silurian to the end of the Palaeozoic.

The K-bentonites indicate a fairly continuous outpouring of silicic pyroclastic material through Llandovery, Wenlock and part of the Ludlow. The fine-grained nature of the beds and the lack of accompanying ash-fall tuffs and other proximal lithologies indicate a distant source region. Magmatic and tectonic discrimination diagrams can be used to infer original magma composition and source volcano settings relative to plate margins. Trace elements with bulk distribution coefficients <1 are partitioned into the liquid phase during partial melting and into the residual liquid of a crystallizing magma. Of these, Th, Ta, Hf, Zr, Ti, Nb, REE and Y are useful for discrimination diagrams. Immobile element chemistry suggests a destructive plate margin calcalkaline setting for all Silurian K-bentonites. Most samples range from dacite to rhyolite in composition on tectonomagmatic discrimination diagrams. The lack of intermediate or basic associated volcanics together with the relatively low HFS element content of the K-bentonites would indicate that they represent the highly evolved products of fractional crystallization, most likely of upper mantle basalts, with some evidence of crustal contamination.

Introduction

The Silurian successions in northwestern Europe contain at least 150 discrete K-bentonite beds produced by explosive volcanism. Of these, the best documented beds occur in Great Britain where more than 100 separate exposures have been described (Huff & Morgan 1990; Merriman & Roberts 1990; Huff et al. 1991; Romano & Spears 1991; Batchelor & Clarkson, 1993), although those in Sweden, Norway, Denmark and Estonia have also been subjected to numerous investigations (Jürgenson 1964; Hagemann 1966; Snäll 1978; Bergström et al. 1992; Sun & Huff, 1995). From North America, in contrast, less than 10 Silurian K-bentonites occurring in the Great Lakes region (Stose & Jonas 1927; Harrison 1991) plus several in Nova Scotia (Boucot et al. 1974) and Manitoulin Island (Johnson 1981) have been recorded. The distribution in time and space of Silurian K-bentonites can provide valuable evidence regarding patterns of tectonism associated with the closing of the Iapetus Ocean and subduction of oceanic crust, and they can serve as event markers useful in the regional interpretation of Silurian stratigraphy (Merriman & Roberts 1990; Bergström et al. 1992).

Facies changes, lack of definitive biostratigraphic control, and the varying effects of diagenesis and low-grade metamorphism all contribute to the difficulties of understanding lateral relations between these beds. The regional distribution of Silurian K-bentonites in northern Europe strongly suggests the possibility of one or more common source areas and thus the possibility that at least some of the K-bentonites could serve as regional marker horizons for event-stratigraphic purposes. Such geologically instantaneous beds are potentially ideal time lines provided they can be distinguished from one another. Quantitative stratigraphic methods, including chemical fingerprinting, can be used to recognize individual beds over great distances (Kolata et al. 1987). In such studies the availability of well-established biostratigraphic zonation in a type or reference area can strengthen the confidence with which regional correlations are made. Careful documentation of the geochemical and mineralogical characteristics of these reference beds is essential to the recognition of the often subtle distinctions between individual beds (Goldman et al. 1994). The selection of these characteristics requires careful consideration of the post-depositional history of the ash beds and the identification of primary chemical and mineralogical features that are sufficiently invariant to serve as useful stratigraphic parameters. Ideal biozones should contain cosmopolitan fauna that are insensitive to changes in facies from deep to shallow marine, and turbidite to carbonate platform environments. Neither graptolite nor conodont zonation is yet capable of providing that critical framework, thus work has recently focused on isotopic studies of apatite and zircon grains (Samson et al. 1989; Tucker et al. 1990) and analyses of melt inclusions in quartz (Delano et al. 1994) as additional ways of fingerprinting K-bentonite beds.

We report here on the stratigraphic, tectonic, mineralogical, and geochemical features of Silurian K-bentonites in the Welsh Borderland. This region has been the focus of intense study of K-bentonites because it contains a wide variety of depositional environments, primarily associated with the Welsh Basin and its depositional history, and also a succession of early and middle Silurian ash beds which could potentially serve as marker horizons throughout the region.

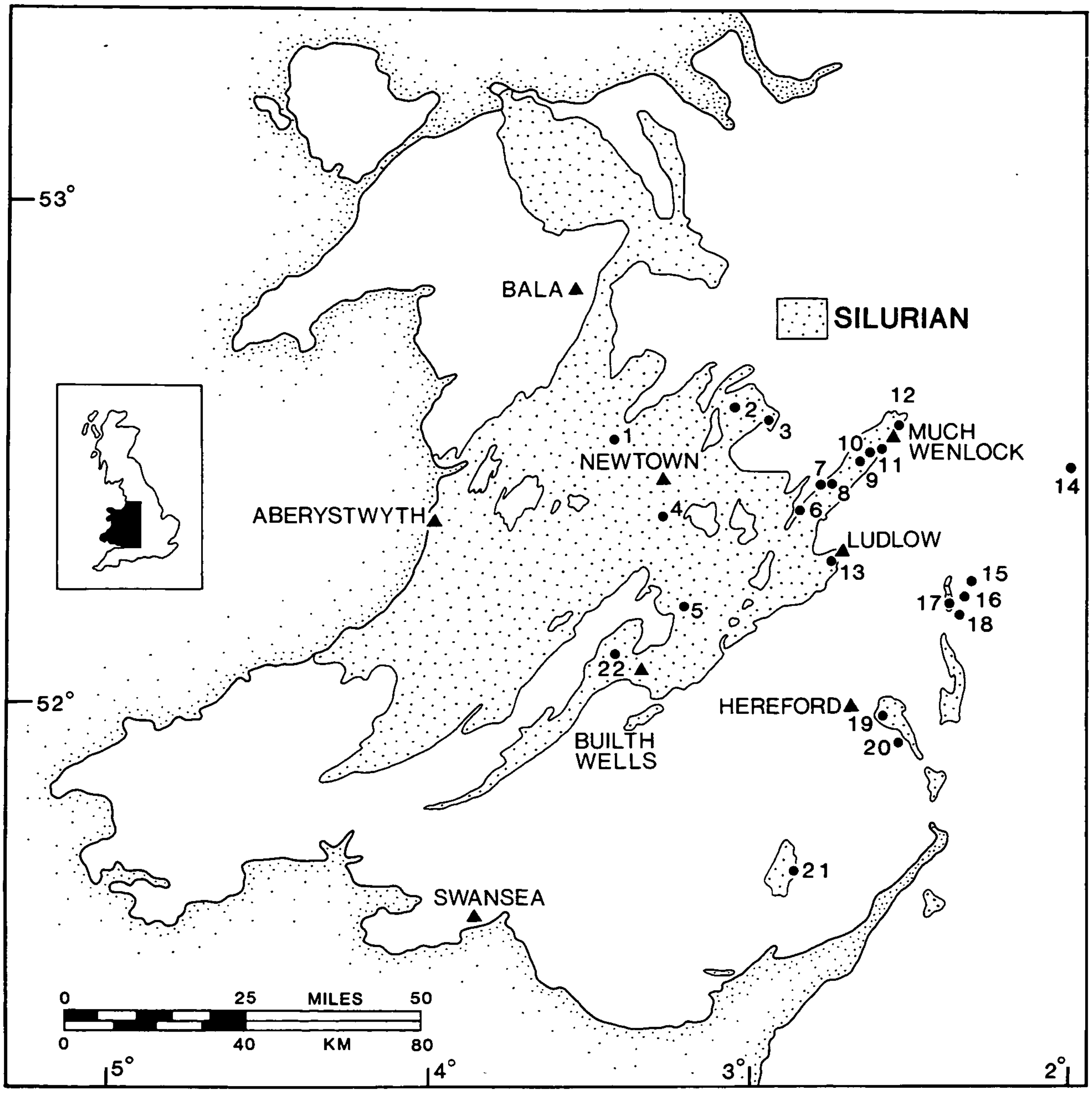

Figure 1. K-bentonite sample localities in the Welsh Borderlands. Bracketed numbers are equivalent designations from Srodoń et al. (1986) 1. Tan-y-Fael, 2. Buttington, 3. Etsell, 4. Newtown, 5. Penybont, 6. Onny R., 7. Eaton, 8. Up. Millichope, 9. Coates Quarry, 10. L. Hill Farm, 11. Leasowes Farm, 12. Gleedon Hill Quarry [M10], 13. Mortimer Forest, 14. Manor Farm [M9], 15. Shavers End [M8], 16. Wallhouse Plantation [M7], 17. Woodbury Quarry [M5], 18. Penny Hill [M4], 19. Woolhope Inlier [M2, M3], 20. Dean's Place, 21. Llangibi Castle [M1], 22. Hafod Yr Ancr.

Samples

Approximately 2 kg samples of K-bentonite were collected from well-documented sections (Fig. 1) in order to take advantage of supporting studies by other workers (see locality register, Appendix A). Initial sampling was done in the type Ludlow Series described by White & Lawson (1978), and the type Wenlock Series described by Bassett et al. (1975). A particular effort was made to collect as many of the K-bentonites described in these type sections as possible. In the Mortimer Forest section samples are designated, wherever possible, by the collection numbers referred to by White & Lawson (1978). Those beds whose identities were not readily correlated with the published description of the section were given unique sample numbers and included in the data set. The Lower Hill Farm Borehole described by Bassett et al. (1975) contains numerous K-bentonites which were

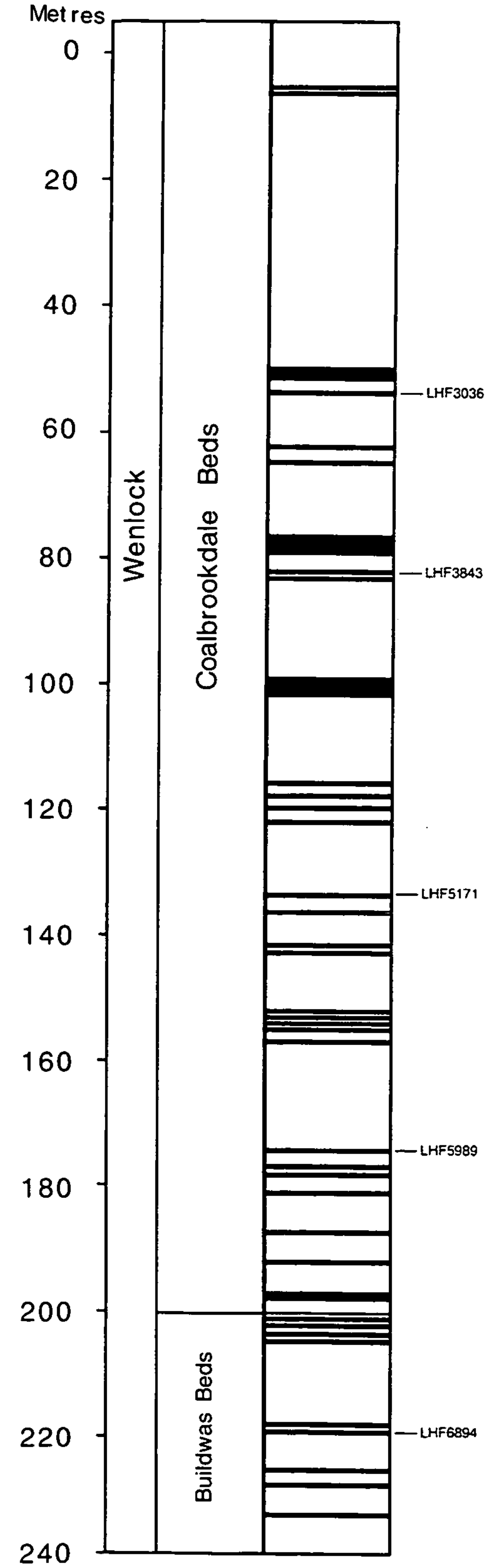

Figure 2 Stratigraphic position of K-bentonite beds in the Lower Hill Farm Borehole (SO 5817 9788), Shropshire. For faunal and lithologic information see Bassett et al. (1975). The thickness of the sections is given in metres on the left and sample numbers refer to analysed beds described in the text.

sampled at intervals to provide some indication of vertical chemical and mineralogical variability in the section (Fig. 2). We further sampled sections described by Teale & Spears (1986) in the Woolhope inlier (Fig. 3), Morgan (1978) and Watkins (1981) at Woodbury Quarry in the Abberley Inlier (Fig. 4), Trewin (1971) in Coates Quarry, plus various localities described by Ross et al. (1982), Środon et al. (1986), Davies et al. (1978) and Morgan (1974).

All samples are well-constrained by biostratigraphic information so that their positions with respect to Stage boundaries are known.

Methods

Clay samples were prepared for powder X-ray diffraction (XRD) analysis by gravity separation of the <2 μm size fraction and sedimentation on glass substrates by the pipette method to achieve oriented clay aggregates. Air-dried and ethylene glycol solvated slides were scanned from 2° to 32°2Θ on a Philips diffractometer with Cu-Kα radiation at a scan rate of 0.25° 2Θ/min. Quantitative estimation of illite and smectite in mixed-layer illite/smectite (I/S) was made using the computer program NEWMOD (Reynolds 1985).

Age determination of the illite in I/S was made by K-Ar measurements on the <0.5 μm size fraction of the clay separates. Samples were separated by centrifugation, flocculated, and dehydrated to provide 2-5 g of material. Potassium was analysed in duplicate using mixed-acid digestion followed by flame photometry with lithium as the internal standard. The minimum error of ±1% was based on replicate analyses of standards. For poorly reproducible samples extra analyses were performed and the quoted error is the standard error of the mean of the determinations. Argon was analysed by the isotope dilution method using an enriched 38Ar spike in a VG-Isotopes MM1200 mass spectrometer and argon extraction line. Analyses of standard glauconite GL-0 yielded 25.08 nl/gm 40Ar and 6.64% K_2O, compared to recommended values of 24.8 and 6.59, respectively. The quoted errors are compounded from errors in the spike calibration and the isotope ratio measurements, and incorporate any error enhancement due to correction for atmospheric argon contamination. Constants used in the age calculations are as recommended by Steiger & Jager (1978).

Seventy-nine bulk samples were analysed for 48 major and trace elements by instrumental neutron activation analysis (INAA) and X-ray fluorescence spectroscopy (XRF). The samples were dried overnight at 60°C and approximately 50 g ground in a shatterbox to <400 mesh.

a.

b.

Figure 3 K-bentonite occurrences in the Woolhope Inlier. (a) Bed SI-47, of Homerian age, is the inclined bed in the centre of the photo (SO 5718 3690). (b) Vew of the Bringewoodian section in Perton Quarry (SO5945 3983). Bed SI-50 occurs at the top of the prominent bench.

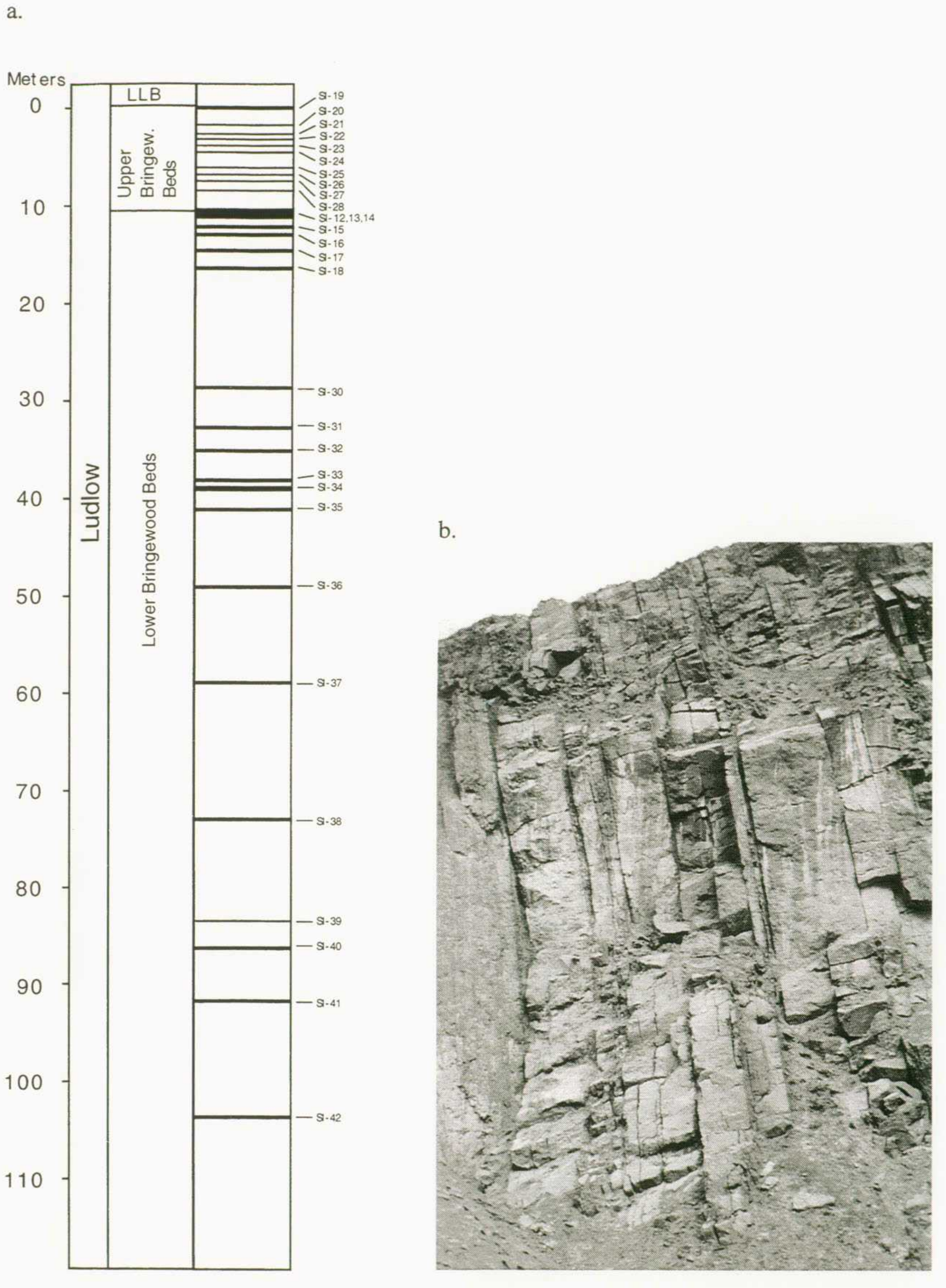

Figure 4 (a) Stratigraphic column of the section at Woodbury Quarry (SO 7404 6354) described by Morgan (1978) showing the position of K-bentonite beds. The thickness of the sections is given in metres on the left and sample numbers refer to analysed beds described in the text. (b) Photo of some of the closely-spaced Upper Bringewood K-bentonite beds in the near-vertical sequence at Woodbury Quarry. Each bedding plane is marked by a single ash fall.

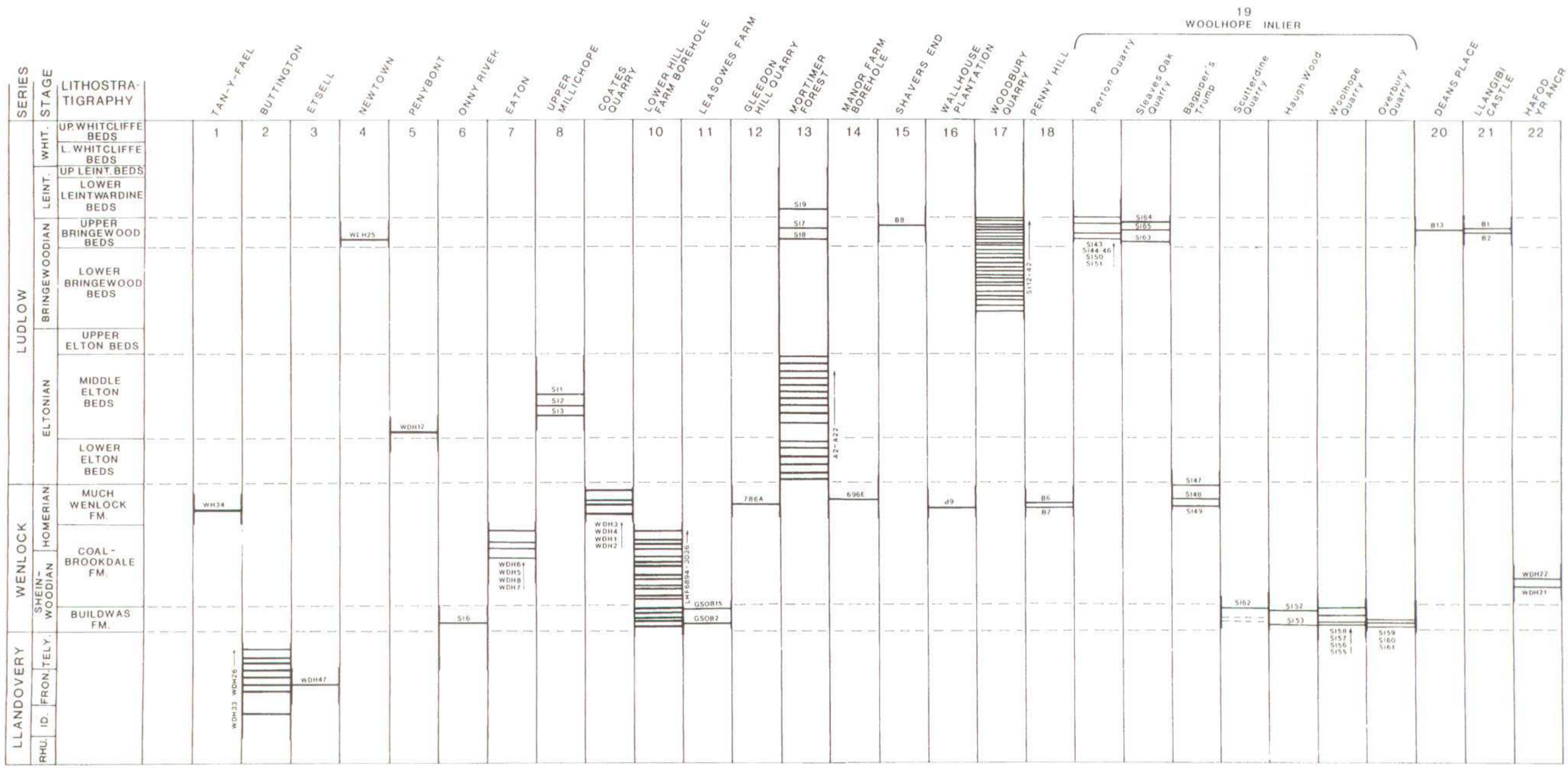

Figure 5 Stratigraphic distribution of Silurian K-bentonites of the Welsh Borderland. Numbers at the top of each column refer to map locations in Figure 1. See Appendix A for additional locality information.

Stratigraphic distribution and field characteristics

More than 100 K-bentonite beds have been identified in Llandovery, Wenlock and Ludlow strata of the Welsh Borderlands; however, very few of them show evidence of continuous preservation beyond the outcrop scale (Fig. 5). This apparent lack of lateral continuity may be due to localized preservation as a function of the frequent facies changes associated with the complex tectonic and sedimentologic history of the Welsh Basin. Transitions from platform carbonate to slope turbidite and hemipelagic shale environments occur within a few tens of kilometers. By contrast, single K-bentonite beds can be traced for over 1500 km in the Middle Ordovician platform carbonates of the eastern Midcontinent of North America where at times a single facies persisted over several tens of thousands of km^2 (Kolata et al. 1987; Haynes 1994). Similar conditions prevailed at the same time in Baltoscandia (Bergström 1989). In the Welsh Basin K-bentonite sequences are preserved discontinuously in sediments including deep water Llandovery Purple Shales, the off-lap facies of the Wenlock Series, turbiditic facies of the Welsh Basin, slope facies of the early Ludlow Eltonian Beds, and carbonate platform deposits of mid-Ludlow to late-Ludlow Bringewoodian Beds. The fine-grained nature of the beds and the lack of accompanying ash-fall tuffs and other proximal facies indicates a distant source region. Individual K-bentonite beds range from 2 cm to 1 m in thickness and typically consist of white to greenish-gray plastic clay with minor amounts of volcanogenic non-clay minerals such as zircon, apatite, euhedral quartz and biotite. The K-bentonites record a nearly continuous outpouring of airfall pyroclastic material during much of the Silurian, most likely related to calc-alkaline arc activity associated with subduction of oceanic crust along the Laurentian margin, north of the Iapetus Suture (Thirlwall 1988).

Phenocryst mineralogy

Biotite

Biotite is a common primary magmatic phase in many K-bentonites and ranges from extremely fine-grained disseminated flakes to large euhedral flakes (Fig. 6c) often occurring in distinct bands within some of the thicker beds. Although frequently altered partially or completely to chlorite, some of the beds sampled here have retained fresh biotite. Some of these fresh biotites have given K-Ar ages which are significant for the Ludlovian series (Ross et al. 1982; Odin et al. 1986).

Biotite samples from eight Ludlow K-bentonites were analysed by electron microprobe and the results compared with biotites from calc-alkaline plutonic and volcanic rocks. Biotite flakes were mounted in epoxy and polished with 1 µm diamond paste. Analyses were calculated on the basis of 24 (O, OH, Cl, F) using the computer program MINTAB (Wilde et al. 1991) according to the general mica formula $X_2Y_{4\text{-}6}Z_8O_{20}(OH,F,Cl)_4$, and the results given in Table 1. The volatiles are assumed to account for most of the approximately 5% low summation of total oxides. The X group cations Ca, Na, and K total between 1.7 and 2.0, with K the major constituent. The tetrahedrally coordinated Z group, accounted for by Si and Al, sums very close to the theoretical occupancy of 8.00 for trioctahedral micas.

Figure 7a shows the relationship of biotites from Silurian K-bentonites with biotites from felsic intrusive and volcanic rocks. The compositions coincide with data reported in the literature and suggest a dacitic to rhyolitic composition for the parent ash. Fe^{2+} and Mn^{2+} enrichment relative to Mg^{2+} is characteristic of biotites from high-silica and K-rich members of the calc-alkaline association. The mean cationic $Mg/(Mg+Fe^{2+})$ for Silurian K-bentonite biotite samples is 0.59, which compares favourably with that of 0.42 for granitic biotites reported by Dodge et al. (1969), 0.65 for the Fish Canyon Tuff (Whitney & Stormer 1985), 0.67 for the Castle Hayne bentonite (Nusbaum et al. 1988), and 0.45-0.5 for the Bishop Tuff (Hildreth 1977). When the data are plotted on the Fe-Mg-Al biotite discrimination diagram of Abdel-Rahman (1994) they fall mainly in the region characterized by calc-alkaline orogenic complexes formed within subduction-related environments (Fig. 7b).

Other minerals

Primary quartz crystals occur commonly in Silurian K-bentonites of the Borderland region. Many features of the quartz grains of the K-bentonites are diagnostic of volcanic origin. The high-temperature beta-form quartz habit (hexagonal bipyramids with no prism faces) is common, and many grains show evidence of magmatic corrosion (Fig. 6d). Some grains also show linear surface features, emanating from a wedge-shaped edge or, more commonly, from a pointed intersection of faces (Fig. 6e,f). These could represent glass spherule trails which formed on the quartz grains immediately after eruption as a result of their rapid rise through a cloud of fine glassy dust.

Apatite occurs in the K-bentonite beds as clear, stumpy euhedral prisms, often with broad tubular cavities running the whole length of the crystal (Fig. 6a). Melt inclusions and inclusions of zircon are sometimes present. Discrete zircon occurs as doubly terminated slender prisms (Fig. 6b). Plagioclase feldspar (andesine-oligoclase) is common, grains often begin replaced by carbonate. No sanidine has been identified from any of the beds.

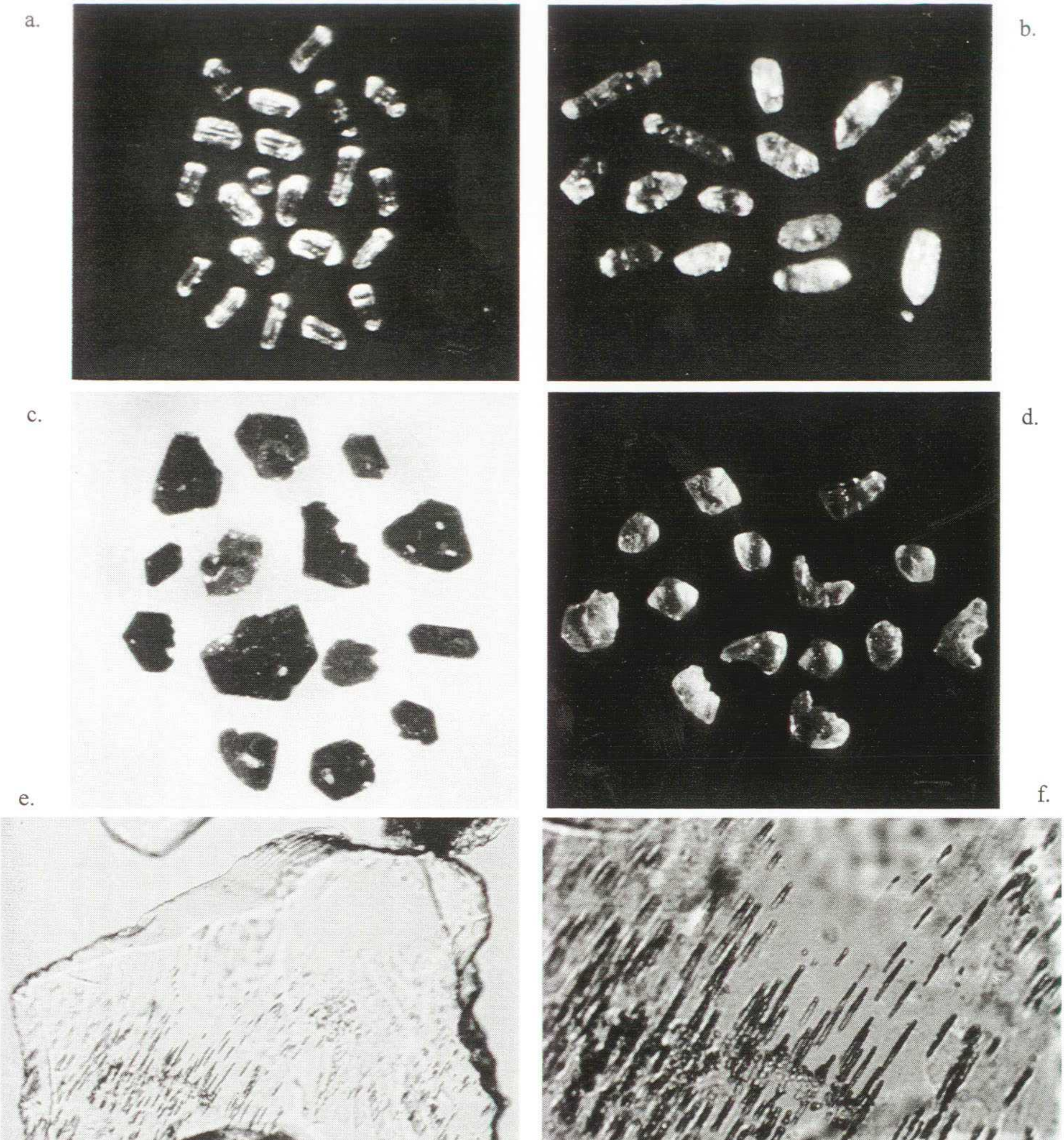

Figure 6 (a) Stumpy euhedral crystals of apatite, some with hollow inclusions running the length of the crystal (oblique incident light, x40). (b) Doubly terminated prismatic crystals of zircon (oblique incident light, x80). (c) Biotite flakes showing euhedral form, occasional embayed outline and presence of apatite inclusions (oblique incident light, x30). (d) Quartz grains showing beta-quartz habit and evidence of magmatic corrosion (oblique incident light, x40). (e) Linear surface features on quartz grains (transmitted light, x300). (f) Detail of (e).

Table 1 Biotite structural formulae

Sample	SI-1	SI-12	SI-24	SI-37	SI-20B	SI-27	SI-31	SI-50A
SiO2	36.74	37.59	37.96	37.92	36.79	36.01	34.78	36.6
Al2O3	13.92	12.55	13.17	13.22	14	16.5	13.77	13.56
Fe2O3	1.83	2.24	2.21	1.97	2.49	3.22	3.25	2.6
FeO	11.01	13.45	13.23	11.81	14.93	19.3	19.5	15.63
MgO	15.43	14.02	14.59	15.72	12.25	6.52	9.74	11.83
CaO	0	0.17	0.14	0	0.11	0.03	0.04	0.01
Na2O	0.71	0.4	0.42	0.59	0.54	0.37	0.32	0.59
K2O	8.55	8.99	8.65	8.83	8.18	8.07	7.29	8.65
TiO2	6.46	4.55	4.59	4.3	4.11	4.52	4.23	5.89
MnO	0.19	0.36	0.31	0.33	0.38	0.23	0.43	0.3
Cr2O3	0	0	0	0	0	0.03	0	0.02
NiO	0	0.02	0.02	0	0	0.05	0	0.03
CalcTotal	94.84	94.34	95.29	94.69	93.78	94.85	93.35	95.71
OxNum	24	24	24	24	24	24	24	24
Si	5.942	6.2	6.165	6.162	6.121	6.031	5.957	6.013
4Al	2.058	1.8	1.835	1.838	1.879	1.969	2.043	1.987
6Al	0.596	0.64	0.687	0.695	0.866	1.289	0.737	0.639
Fe3	0.223	0.278	0.27	0.241	0.312	0.405	0.419	0.322
Fe2	1.489	1.855	1.798	1.605	2.078	2.704	2.793	2.147
Mg	3.721	3.447	3.533	3.808	3.038	1.628	2.487	2.898
Ca	0	0.03	0.024	0	0.02	0.005	0.007	0.002
Na	0.223	0.128	0.132	0.186	0.174	0.12	0.106	0.188
K	1.764	1.892	1.792	1.83	1.736	1.724	1.593	1.813
Ti	0.786	0.564	0.561	0.525	0.514	0.569	0.545	0.728
Mn	0.026	0.05	0.043	0.045	0.054	0.033	0.062	0.042
Cr	0	0	0	0	0	0.004	0	0.003
Ni	0	0.003	0.003	0	0	0.007	0	0.004
Oct	6.839	6.833	6.891	6.918	6.862	6.627	7.042	6.775
Int	1.987	2.05	1.948	2.017	1.93	1.849	1.706	2.003

Clay mineralogy

Powder X-ray diffraction scans indicated that all K-bentonites are characterized by interstratified illite/smectite (I/S) with ordering ranging from R0 (random interstratification) to R3 (long-range ordered interstratification) (Table 2). Representative examples are shown in Figure 8. For glycol-treated samples the presence of a single diffraction maximum near 5°2Θ is indicative of R0 ordering. The appearance of short-range R1 ordering is indicated by a superlattice peak between 2-3°2Θ, and R3 ordering is revealed by the presence of two closely-spaced reflections near 9°2Θ (Reynolds, 1980). Kaolinite occurs as an accessory component in many Llandovery and Wenlock samples, but is not present in Ludlow K-bentonites. I/S ordering and the related percent of the illite component does not follow any systematic pattern of distribution with respect to depth of burial or facies. For example R0, R1 and R3 ordering occurs in K-bentonites in the Buildwas Formation shelf carbonates from the Woolhope Inlier as well as the deep marine purple Llandovery shales exposed at Buttington.

Lattice fringe images obtained by high resolution transmission electron microscopy (HRTEM) reveal the R>1 samples are dominated by crystallites which display 20Å, 30Å, and 40Å spacings (Cetin & Huff, 1995). These units represent ordered illite and smectite layers and are consistent with computer simulation results from earlier studies. Lattice fringe images of samples exchanged with alkylammonium ions show that the expanded interlayers between the illite packets are predominantly 15-16Å thick, indicating a monolayer-to-bilayer arrangement of alkylammonium ions. This is a characteristic feature of high-charge (0.45-0.6) smectite as well as low-charge (0.6-0.7) vermiculite (Lagaly & Weiss, 1976; Lagaly, 1982). R3 samples have alkylammonium ion exchange characteristics which indicate layer charges equivalent to high-charge vermiculite (Cetin & Huff, 1995).

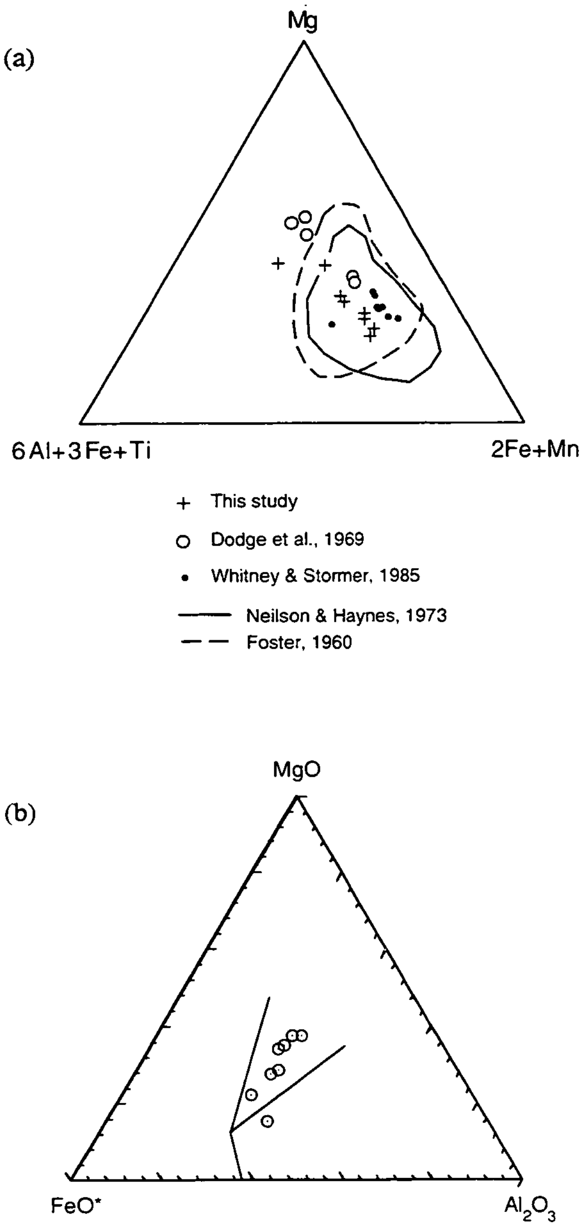

Figure 7 Silurian K-bentonite biotite composition compared with published analyses of biotites from tuffs, granites, granodiorites, monzonites, monzodiorites, quartz diorites, and diorites. (a) As with both plutonic and volcanic-derived biotites these show a range in compositions with respect to Mg/(Mg+Fe) ratios. They compare favourably with felsic tuffs such as the Fish Canyon Tuff and the Eocene Castle Hayne bentonite. (b) Plotted on the Fe-Al-Mg discrimination diagram of Abdel-Rahman (1994) the data fall mainly in the category of calc-alkaline orogenic complexes.

Many K-bentonite samples used in this study contain discrete illite and chlorite in addition to I/S, and in some cases these phases dominate the bed mineralogy (Table 2). Their distribution, however, tends to be site-specific - i.e. related more to particular localities than to stratigraphic intervals - and strongly suggests an origin related to sedimentary conditions in those environments. Romano & Spears (1991) reached a similar conclusion on the basis of the presence of chlorite. The Bringewoodian section at Woodbury Quarry (Fig. 3a) contains 30 K-bentonite beds, of which three contain I/S as the only clay mineral (Morgan 1978) while the others have varying amounts of additional illite and chlorite. The chlorite could be a by-product of burial metamorphism during the conversion of smectite to illite, but detrital illite could be expected to be destroyed at the same time (Hower et al. 1976). Moreover, the I/S in the Woodbury Quarry K-bentonites has R0 and R1 ordering and thus shows no evidence of the thermal effects accompanying deep burial. Kaolinite is not a common detrital component in the K-bentonites and may have formed diagenetically through the alteration of K-feldspar. X-ray diffraction patterns show it to be well crystallized and it occasionally occurs as the only other clay mineral besides I/S. Kaolinite is restricted to Llandovery and Wenlock strata and does not occur in Ludlow K-bentonites except in rare, trace amounts.

Anchizonal metamorphism has converted Silurian K-bentonites to I/S with about 95% I in the Southern Uplands (Merriman & Roberts 1990) and north Yorkshire (Romano & Spears 1991) and maximum temperatures in these areas are estimated to have been of the order of 300^{0}C. Under very low-grade metamorphic or diagenetic conditions, however, geochemical factors are more likely to play a decisive role in controlling I/S ratios, particularly the behaviour of fluid flow. Illitization has been closely linked to periods of tectonism and basin deformation during which gravity-driven fluids mobilize available cations and increase their activity with respect to clay mineral structural exchange sites (Elliott & Aronson 1987). We investigate this aspect further by measuring K-Ar ages of the illite component of K-bentonite I/S and discuss the results below.

Table 2 Clay mineralogy of UK Silurian K-bentonites

Sample	Clay min	R(I/S)	%I	Sample	Clay min	R(I/S)	%I	Sample	Clay min	R(I/S)	%I	Sample	Clay min	R(I/S)	%I
LUDLOW				LUDLOW				WENLOCK				LLANDOVERY			
Bringewoodian				Eltonian											
SI-8 (C-2)	I/S	1	74	A17/A18	I/S	1	61	GSO-B15	I/S + K	1	60	WDH-27	I/S (+K)		
SI-9 (C-12)	I/S	1	70	A2	I/S			GSO-B2	K (+tr Ch, I, I/S)			WDH-28	I/S		
SI-12	I/S	1.5	82	A22	I/S			SI-47	I/S	2	85	WDH-29	I/S		
SI-13	I/S + I + Ch			A3/A4	I/S (+I)			SI-48	I + Ch			WDH-30	I/S		
SI-14	I/S + I + Ch + K?			A8/A9	I/S			SI-52	I/S + K	1	73	WDH-31	I/S	2	85
SI-15	I/S + (I + Ch)			SI-1	I/S	1	77	SI-53	I/S	1	70	WDH-32	I/S + K		
SI-16	I/S + I + Ch			SI-2	I/S	1	75	SI-55	I/S	0	40	WDH-33	I/S + K		
SI-17	I/S + I + Ch			SI-3	I/S	1	78	SI-56	I/S + (K)	0.5	50	WDH-47	I/S	1	75
SI-18	I/S + I + Ch			SI-10 (A4/A5)	I/S	1	75	SI-57	I/S + K	1	73	SI-6	I/S + K	1	70
SI-19	I/S + I + Ch + K?			SI-11 (A5)	I/S	1.5	78	SI-58	I/S + K	1	75				
SI-20	I/S + I + Ch + K			SI-63	I/S (+I)	0	48	SI-59	I/S	0	40				
SI-21	I/S + I + Ch			SI-65	I + I/S			SI-60	I/S + I (+K)	0	35				
SI-22	I/S + I + Ch + K?			WDH-12	I/S			SI-61	I/S + K	1	80				
SI-23	I/S + I + Ch + K							SI-62	I/S + I + Ch?	1	80				
SI-24	I/S + I + Ch + K							WDH-1	I/S	1	75				
SI-25	I/S + K?							WDH-2	I/S + K						
SI-26	I/S + I + K + Ch?							WDH-3	I/S (+I)						
SI-27	I/S + I + Ch							WDH-4	I + Ch (+I/S)						
SI-28	I/S + I + Ch + K							WDH-5	I/S (+I)						
SI-30	I/S + I + Ch							WDH-6	I + Ch + I/S						
SI-31	I/S + I + Ch + K							WDH-7	I/S (+K)						
SI-32	I/S + I + Ch +K?							WDH-8	I/S (+K)						
SI-33	I/S + I + Ch + K							WDH-21	I + CH (+I/S?)						
SI-34	I + Ch + I/S (tr)							WDH-22	I + Ch (+I/S?)						
SI-35	I/S + I + Ch + K?							WDH-25	I/S	3	95				
SI-36	I/S + I + Ch + K?							WH-34	I/S	3	95				
SI-37	I/S + I + Ch							LHF-3036	I/S + K	1.5	71				
SI-38	I + Ch + I/S (tr)							LHF-3843	I/S + K	0	61				
SI-39	I/S + I + Ch (tr)							LHF-5171	I/S + K	1.5	75				
SI-40	I/S + I + Ch							LHF-5989	I/S + K	1.5	67				
SI-41	I/S + I + Ch														
SI-42	I/S + (Ch + I)														
SI-44	I/S + K (tr)	1	60												
SI-46	I/S + (I + K)	0	30												
SI-50A	I/S	0.5	68												
SI-51	I/S + I + Ch	0													
SI-64	I/S	0.5	50												

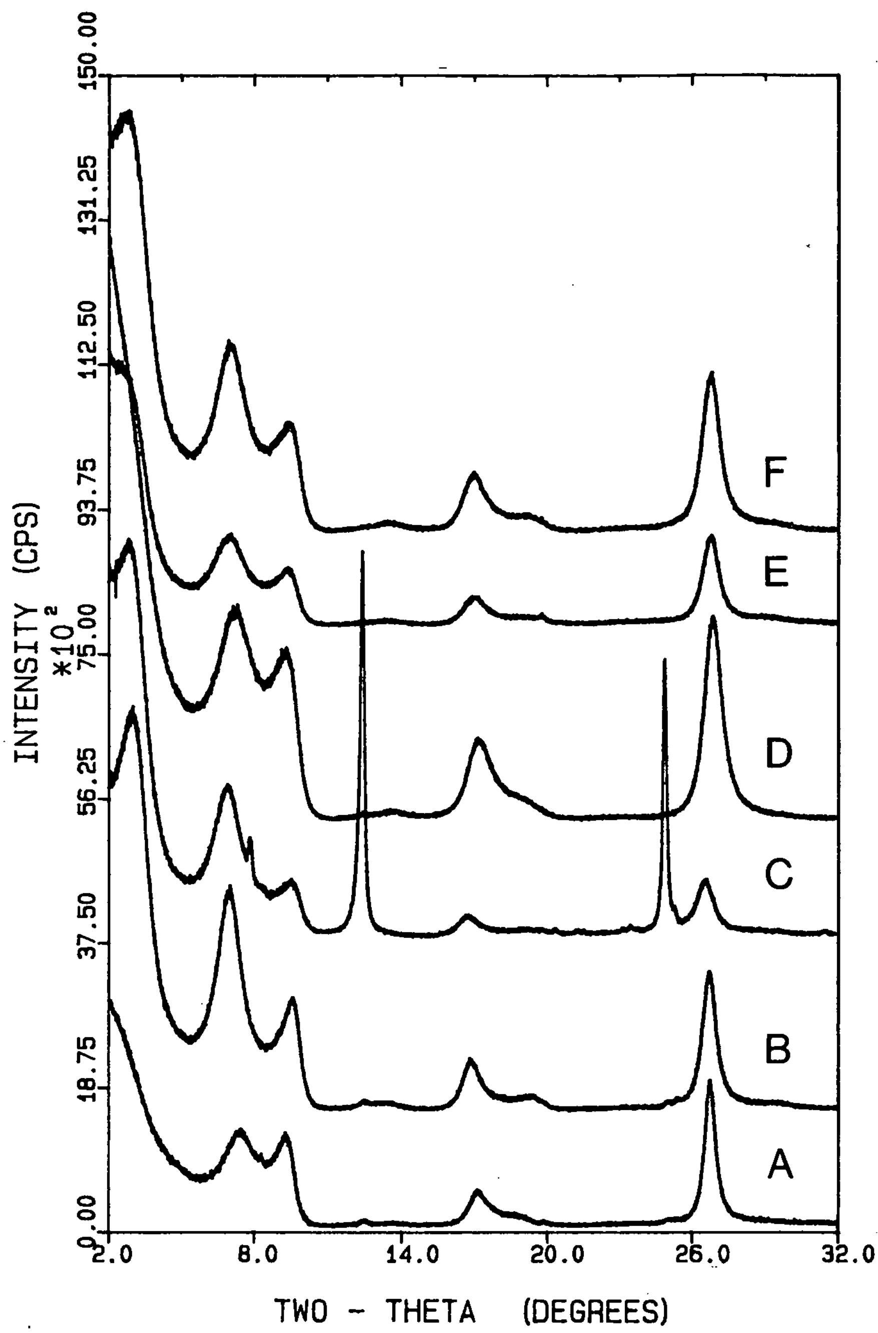

Figure 8 Selected powder XRD tracings of the <2 μm size fraction showing short-range (R1) and long-range (>R1) ordered I/S. Kaolinite occurs commonly in Llandovery and Wenlock samples but is absent in Ludlow samples. Llandovery: A = >R1, 80% I; B = R1, 67% I; Wenlock: C = R1, 65% I; D = >R1, 80% I; Ludlow: E = R1, 75% I; F = R1, 74% I.

Illite K-Ar age determination

The chemistry of I/S clays from Silurian K-bentonites in the UK was studied in detail by Drodon et al. (1986) who reported a strong positive correlation between the amount of fixed K and the percent I in I/S for the range 10-40% S. Fixation of K is affected by the increased substitution of Al for Si in the tetrahedral sheet of the smectite component and the consequent increase in total layer charge. Studies of I/S by alkylammonium ion exchange experiments have demonstrated the presence of two distinct mineral phases in I/S from K-bentonites, one a low-charge smectite-like form and the other a high-charge illite (Cetin & Huff 1995). Thus, one well-documented model of I/S formation invokes the transformation of

Table 3 K-Ar ages of illite in Silurian K-bentonites

Sample	Stratigraphy	Ma**	%K ± CV	% Atmos. 40Ar	Rad. 40Ar (nl/g) ± CV	Age (Ma) ± 2 s
		410				
M1*	Lud.		5.48 ± 1.0	6.6	67.95 ± 1.01	293 ± 6
SI11	Lud.		4.59 ± 1.0	27.9	60.54 ± 1.09	311 ± 9
SI50A	Lud.		3.93 ± 1.0	39.4	52.99 ± 1.21	317 ± 9
SI12	Lud.		5.07 ± 1.0	13.1	70.21 ± 1.03	325 ± 9
M5*	Lud.		5.09 ± 1.0	8.4	71.06 ± 1.01	329 ± 6
M8*	Lud.		6.02 ± 1.0	3.5	88.68 ± 1.00	341 ± 6
		424				
M10*	Wen.		4.46 ± 1.0	23.5	37.23 ± 1.06	205 ± 4
WDH1	Wen.		3.78 ± 1.0	36.7	32.42 ± 1.17	206 ± 5
GSOB15	Wen.		3.56 ± 1.5	46.5	32.23 ± 1.33	217 ± 6
LHF3843	Wen.		1.15 ± 3.2	56.4	12.53 ± 1.78	260 ± 18
LHF5171	Wen.		3.61 ± 1.0	24.1	40.88 ± 1.06	270 ± 7
LHF5989	Wen.		3.93 ± 1.0	22.7	45.10 ± 1.07	273 ± 7
LHF3036	Wen.		3.06 ± 2.2	26.4	34.77 ± 1.10	275 ± 15
M4*	Wen.		5.18 ± 1.0	19.0	61.38 ± 1.04	280 ± 6
M3*	Wen.		1.95 ± 1.0	22.1	24.52 ± 1.05	303 ± 6
M7*	Wen.		5.28 ± 1.0	5.6	69.29 ± 1.01	311 ± 6
SI56	Wen.		2.78 ± 1.0	29.8	37.73 ± 1.09	319 ± 9
M9*	Wen.		3.98 ± 1.0	28.7	54.19 ± 1.08	325 ± 7
SI47A	Wen.		4.37 ± 1.0	24.8	60.49 ± 1.10	325 ± 9
M2*	Wen.		4.60 ± 1.0	9.6	67.60 ± 1.02	343 ± 6
M11*	Wen.		6.84 ± 1.0	5.3	106.0 ± 1.01	360 ± 9
WH34	Wen.		6.53 ± 1.0	19.9	106.6 ± 1.03	378 ± 9
SI6	Wen.		2.99 ± 1.0	49.4	42.64 ± 1.43	333 ± 11
		430				
WDH31	Llan.		5.74 ± 1.0	16.5	92.21 ± 1.03	372 ± 10
WDH47	Llan.		4.61 ± 1.0	14.4	67.12 ± 1.04	374 ± 10
		439				

* Samples described in Środon et al. (1986)

** Depositional ages taken from Harland et al. 1990.

CV = % standard deviation

smectite to illite by increased layer charge and the consequent fixation of K. Illite has been shown to be an excellent K-Ar clock below the blocking temperature of Ar (Aronson & Lee 1986), and for higher-temperature regimes K-Ar age determination has been used to constrain the onset of closure of the Ar system and related tectonic uplift in the Southern Uplands (Huff et al. 1991).

The <0.5 μm size fractions of 25 Llandovery, Wenlock, and Ludlow K-bentonites were dated by K-Ar methods and gave a range of ages from 205±4 to 378±9 Ma for all samples, with a mean of 306±19 Ma (Table 3). Llandovery samples average 373±6 Ma, Wenlock samples average 293±26 Ma, and Ludlow samples average 319±12 Ma.

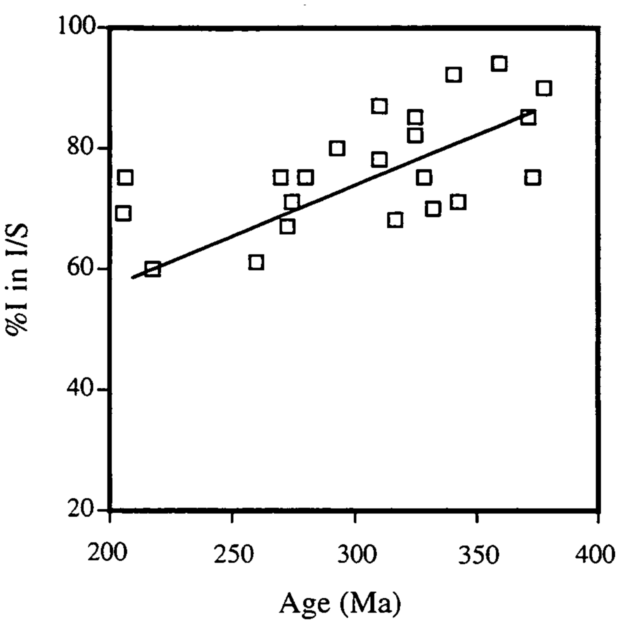

Figure 9 Correlation between K-Ar age of the illite in I/S clay and the percent illite. Despite scatter, some of which is due to the use of different methods of determining %I, the data suggest that these samples, which have not been subjected to metamorphic grade temperatures, have undergone slow, progressive illitization during the middle and late Palaeozoic.

The significance of such a distribution pattern may be viewed in terms of several possible geochemical mechanisms. First, the ages may represent closure temperatures reached during cooling, in which case they would record thermal events in the tectonic history of the Welsh Basin. Regional and vertical distribution patterns would appear to preclude this possibility, however, since there is no apparent relationship between age and location with respect to the basin margin. The four LHF samples are taken from the Lower Hill Farm borehole (Fig. 2). There is a vertical difference of approximately 170 m between the upper and lower samples, with no apparent difference in the illite ages although the Reichweite values range from 0 to 1.5. A second possibility is that particle size has some influence on measured age. Hay et al. (1988) determined K-Ar ages on both coarse (0.2-2.0 μm) and fine (<0.1 μm) fractions of Ordovician K-bentonite and found that the former gave younger ages, on average, by about 15 Ma. The reverse pattern is usually observed (Odin et al. 1986). Hay et al. (1988) suggested that their results might be due to Ostwald ripening, in which crystal size increases through time with dissolution of the fine fraction. The net effect would be to give older ages for small particles and younger ages for the large ones. Our studies were confined to the <0.5 μm fraction and any particle size variation between samples might also be reflected in slight variations in the ages determined, but not to the extent seen in this assemblage. Third, they may reflect the actual timing of potassium metasomatism and the conversion of smectite to illite. Figure 9 shows the relationship between age and percent I in the I/S. The data are scattered, but a weak positive correlation (r^2 = 0.2) can be seen. Some of the scatter in the data may arise from the use of different methods of determining %I in the samples. All M-series samples were taken from Środon et al. (1986) and the %I in that study was determined by graphical methods. The remaining samples were interpreted using NEWMOD which uses a curve-fitting algorithm. When the M-series samples are excluded from the regression analysis the r^2 value is doubled. We consider the data permissive that K-Ar measurements document the gradual illitization of smectite with a 20% increase in illite over more than 150 Ma. In the absence of evidence of low-grade to medium-grade metamorphic temperatures in the Welsh Basin during the Palaeozoic the diffusion reactions responsible for emplacement of fixed potassium were extremely slow.

Chemistry

Whole-rock major and trace element analyses for 37 Ludlow, 32 Wenlock and 10 Llandovery K-bentonites are summarized in Table 4. Huff & Morgan (1990) showed that K-bentonites from this same area could, when grouped by Series and by Stage, be chemically distinguished from one another by means of discriminant analysis, and suggested that chemical fingerprinting used in conjunction with biostratigraphic techniques could enhance the resolution of regional correlation. Tracing of individual beds throughout the region would require a greater population of samples from well-documented K-bentonites than has been possible to date due to the limited availability of outcrops and boreholes, but it has been applied successfully in studies of Ordovician K-bentonites in North America (Kolata et al. 1987) and should, with further study, be applicable in the UK as well. Melt-inclusion chemistry (Goldman et al. 1994) may also prove to be a useful method since it relies less heavily on the statistical analysis of large data sets.

Immobile trace elements and rare earth elements (REE) have been used by numerous workers to provide information on the magmatic composition of parent ashes and tectonic setting of the source volcanoes (Teale & Spears 1986; Huff & Morgan 1990; Merriman & Roberts 1990). These studies have generally relied on the use of empirically-based discrimination plots derived from studies of igneous rocks of known origin, and while not providing

Table 4 Mean major and trace element analyses of Silurian K-bentonites of the Welsh Borderland

Group	**Si**	**Al**	**Ca**	**Mg**	**Na**	**K**	**Fe**	**TI**	**P**
Bringewd. (n=16)	50.84	19.79	3.46	3.10	0.35	4.64	3.06	0.49	0.09
Eltonian (n=21)	47.20	21.47	5.04	2.81	0.32	4.90	2.50	0.61	0.08
Wenlock (n=34)	48.50	23.37	3.44	2.73	0.37	4.29	2.62	0.62	0.09
Llandovery (n=9)	46.47	27.04	2.46	1.47	0.55	5.24	4.10	0.82	0.11

	As	**B**	**Ba**	**Be**	**Bi**	**Br**	**Co**	**Cs**	**Cu**
Bringewd. (n=16)	4.56	135.63	376.88	4.13	0.72	3.35	9.83	12.39	13.66
Eltonian (n=21)	6.19	234.29	310.95	4.05	0.59	4.41	7.53	13.37	17.81
Wenlock (n=34)	6.71	149.91	220.59	3.85	0.51	10.99	10.09	11.41	27.12
Llandovery (n=9)	3.33	161.11	1802.22	4.56	0.33	9.02	9.74	8.32	365.94

	Hf	**Li**	**Mn**	**Nb**	**Ni**	**Pb**	**Rb**	**Sb**	**Sc**
Bringewd. (n=16)	11.23	61.00	216.75	30.31	20.00	27.25	237.50	0.77	11.72
Eltonian (n=21)	13.35	38.60	391.33	19.67	20.43	31.71	220.48	1.07	16.64
Wenlock (n=34)	13.40	99.67	194.53	29.82	27.56	51.71	159.12	1.64	15.00
Llandovery (n=9)	13.66	76.38	986.67	33.33	13.00	21.78	180.00	2.17	14.03

	Se	**Sr**	**Ta**	**Th**	**U**	**V**	**W**	**Y**	**Zn**
Bringewd. (n=16)	3.09	74.53	2.59	33.06	7.13	40.13	11.25	66.25	66.44
Eltonian (n=21)	1.29	141.43	1.94	28.01	7.41	58.38	3.62	92.38	73.29
Wenlock (n=34)	1.37	112.65	2.36	28.65	6.82	40.06	6.82	75.88	104.53
Llandovery (n=9)	0.86	106.67	2.72	29.67	4.09	62.67	8.00	70.00	46.67

	Zr	**La**	**Ce**	**Nd**	**Sm**	**Eu**	**Tb**	**Dy**	**Yb**	**Lu**
Bringewd. (n=16)	379.38	66.03	129.81	54.94	9.76	1.85	1.64	10.49	5.80	0.91
Eltonian (n=21)	486.67	59.90	142.81	67.19	12.37	7.12	1.95	12.47	7.21	1.09
Wenlock (n=34)	449.71	49.35	112.59	51.94	9.66	1.89	1.70	10.66	6.17	0.95
Llandovery (n=9)	534.44	21.32	52.89	21.33	5.35	1.71	1.78	11.53	6.01	0.90

* Values for Si-P are given as weight percent oxides. Values for As-Lu are in ppm.

absolute proof of magmatic origin or affinity, these diagrams serve as useful and important sources of information about the tectonic settings and general magma chemistries, particularly in cases where other geological evidence is ambiguous. For K-bentonites which are the altered remnants of pyroclastic deposits we rely principally on immobile trace elements for information about original magma chemistry. Previous studies have shown that those elements which tend to be unaffected by weathering or that reside in as yet unaltered primary phenocrysts are reliable indicators of past rock history (Teale & Spears 1986; Huff & Morgan 1990; Merriman & Roberts 1990). TiO_2, the high field strength (HFS) elements Zr, Nb, Hf, Ta, and the REE are commonly considered to be immobile under most upper crustal conditions and are thus useful indicators of petrogenetic processes. Nb/Y ratios are a measure of alkalinity and Zr/TiO_2 an index of differentiation. A plot of Zr/TiO_2 against Nb/Y (Fig. 10) after Winchester & Floyd (1977) shows that most Silurian K-bentonites were derived from subalkaline silicic magmas ranging from dacite to rhyolite in composition. Some samples are more alkaline in composition and plot as trachytes and trachyandesites. Many explosively erupted volcanic ashes tend to have moderate to high Nb and Zr content reflective of their silicic and high-volatile (H_2O) character (Izett 1981). The water content of melt inclusions from rhyolitic Middle Ordovician K-bentonites is approximately 5% by weight (Huff et al. 1992) and it is the explosive release of this volatile component that initiates the plinian and co-ignimbrite clouds which transport ash, rock, and pumice fragments over thousands of square kilometers producing the K-bentonite stratigraphic record. Geochemical information concerning the tectonomagmatic origin of K-bentonites is provided by several, widely referenced discrimination plots. In Figure 11 plots of Ta against Yb and Nb against Y show that the majority of Silurian K-bentonites lie in the field of within-plate granites as defined by Pearce et al. (1984). These data suggest the protolith of the granitoid magma may have formed by the partial melting of hydrous crustal rocks (Roberts & Clemens 1993). The silicic nature of Silurian K-bentonites in the UK raises the question of whether the parent magmas were wholly mantle-derived or contain a significant portion of continental crustal material.

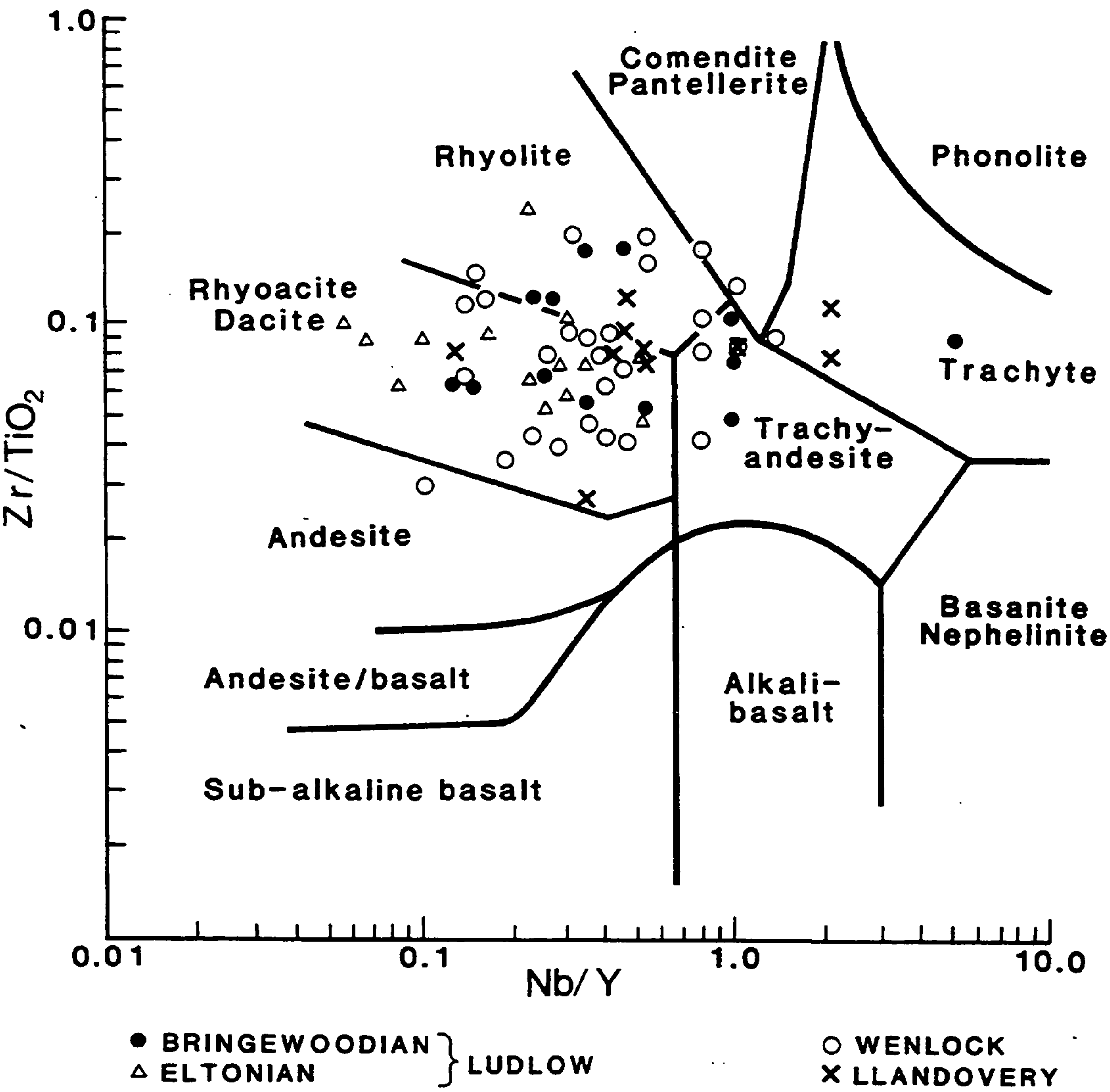

Figure 10 K-bentonite samples plotted on the magmatic discrimination diagram of Winchester & Floyd (1977). Moderate to high proportions of Nb and Zr indicate the original ashes were dacitic to rhyolitic in character.

Many continental margin rhyolites and dacites are associated with basalts, and the bimodal nature of such assemblages can be interpreted as representing the partial melting products of different source materials. Hildreth et al. (1991) presented data for continental crustal rhyolites in the Yellowstone caldera as products of partial melting of hybrid crustal rocks as opposed to fractionates of basaltic parents. Silurian K-bentonites plotted on the Th/Yb vs. Ta/Yb discrimination diagram of Hildreth et al. (1991) show a well-defined clustering around the magmatic arc rhyolites of the Central Andean Arc (Fig. 12). Th/Yb ratios cause the samples to plot just above and parallel to the fractionation trend of mantle-derived basaltic magmas. These K-bentonites do not appear to be associated with any intermediate or mafic volcanics, which would tend to rule out multiple source magmas. They are characterized by a very pronounced depletion of Ta relative to Th and La, high Th/La and Th/Hf ratios, fairly low Zr content, moderate light REE enrichment,

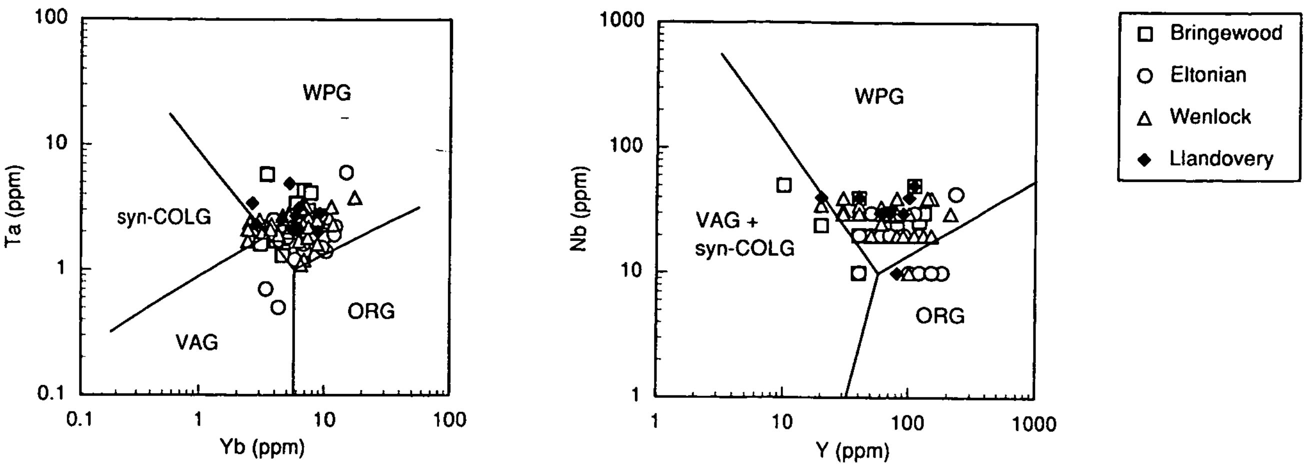

Figure 11 REE elements may be enriched in magmas derived from the fractional crystallization of upper mantle basalts or through modification by partial melting of sediments or continental crustal rocks. Using the discrimination diagrams of Pearce et al. (1984) Silurian K-bentonites plot mainly in the field of within-plate granites. Abbreviations used are: WPG = within-plate granites; ORG = ocean ridge granites; VAG = volcanic arc granites; and syn-COLG = syncollision granites.

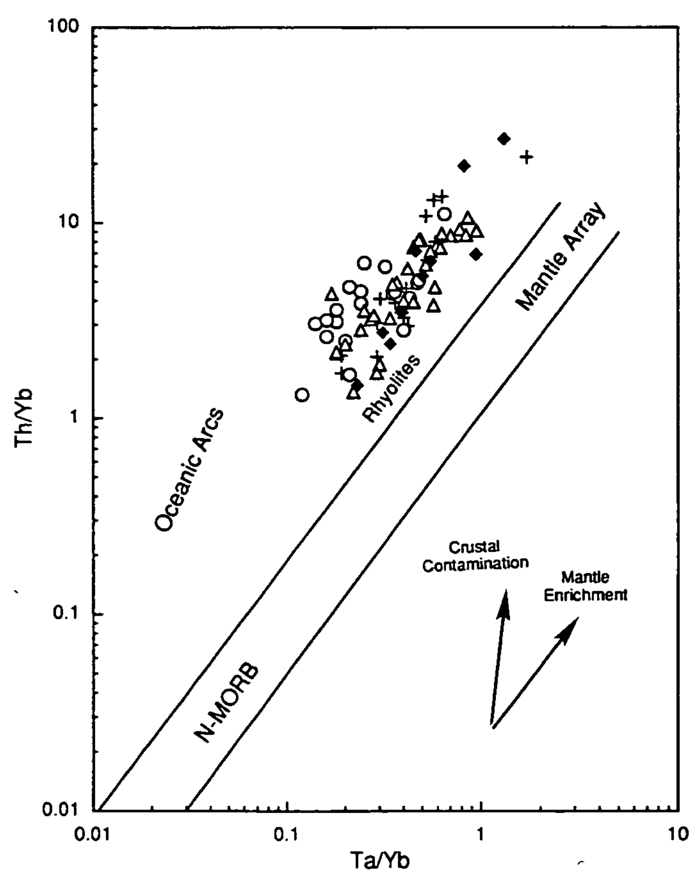

Figure 12 Silurian K-bentonite trace element chemistry compared with a group of Yellowstone rhyolites reported by Hildreth et al. (1991). Slight enrichment in Th suggests some mixing of crustal material, but essentially the data define a trend parallel to the fractional crystallization trend of upper mantle rocks. K-bentonite symbols are the same as in Figure 11.

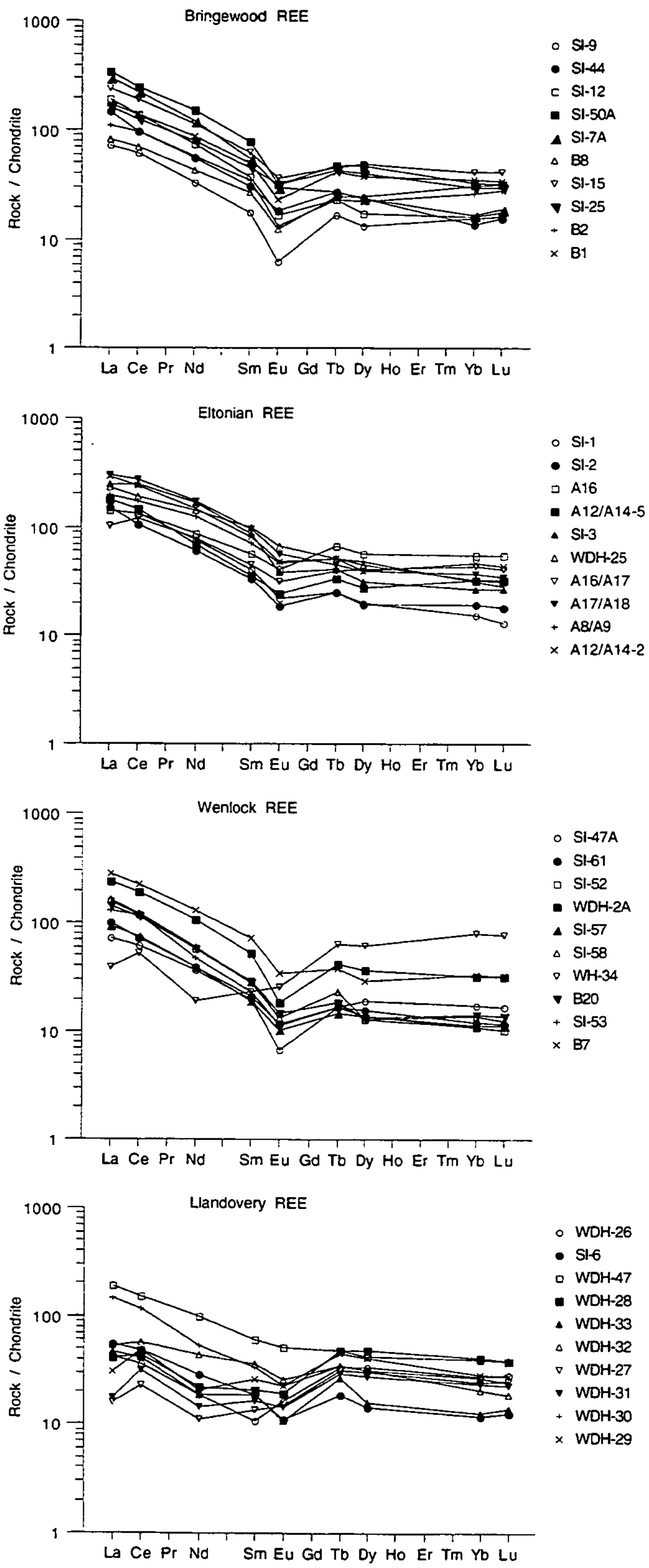

Figure 13 REE ratio plots have moderate to steep slopes reflecting LREE enrichment. Negative Eu anomalies indicate at least partial crystallization of plagioclase. Both features are characteristic of highly evolved calcalkaline magmas erupted in plate margin subduction or collision environments.

and strong negative Eu anomalies. These data argue for a highly fractionated magma erupting in a within-plate extensional setting, possibly related to subduction (André et al. 1986), and possibly augmented by partial melting of some felsic crustal material. A similar conclusion was reached by Huff et al. (1993) for Late Ordovician K-bentonites in the UK, and the Silurian beds may be seen as a continuation of that situation in which explosive volcanism continued into the Ludlow following a Wenlock closure of Iapetus, possibly associated with post-collision transpression.

REE data are shown as chondrite-normalized plots for 40 Silurian K-bentonites in Figure 13. Llandovery samples have relatively flat curves with an overall enrichment of 20-40 times chondritic. The absence of a pronounced negative Eu anomaly and the lack of demonstrable LREE enrichment suggests that these are more intermediate in composition than younger Silurian K-bentonites. Wenlock and Ludlow beds show LREE enrichment approximately 100-300 times chondritic and a moderate to pronounced negative Eu anomaly, indicating removal of plagioclase either by fractional crystallization or winnowing during ashfall. Eu/Eu* is a measure of Eu content relative to other REE such that Eu/Eu* >1 corresponds to a positive anomaly and Eu/Eu* <1 corresponds to a negative anomaly and indicates depletion of Eu. Average Eu/Eu* values are 0.58 for Bringewood beds, 0.73 for Eltonian beds, 0.59 for Wenlock beds, and 0.71 for Llandovery beds. These features are characteristic of more highly evolved subalkaline magmas (Jakes & White, 1972) and resemble previously reported Cambrian, Ordovician and Silurian K-bentonite compositions (Roberts & Merriman 1990; Huff et al. 1992). The lack of correspondingly depleted HREE indicates that fractionation of phases such as garnet and clinopyroxene did not play a major role in the evolution of these calc-alkaline magmas. Light to heavy REE ratios are quite high with the exception of Llandovery samples (c. <10), when plotted as Ce/Yb versus La/Lu (Fig. 14). One exception in an otherwise strongly subalkaline Wenlock suite is sample WH-34 from a basinal turbidite sequence exposed at Tan-Y-Fael in Mid-Wales, generally considered to be Wenlock in age (Cummins 1957). REE patterns of this sample are much more similar to Llandovery samples than to the rest of the Wenlock or Ludlow samples. However, its bulk chemical composition is clearly nearer to known Wenlock K-bentonites than Llandovery beds when examined by discriminant analysis (Huff & Morgan 1990), and this argues in favour of a Wenlock age. The discordant REE pattern of WH-34 and similar-appearing Llandovery samples is more likely due to either post-depositional geochemical changes in the basinal turbidites or, more likely, to sedimentological mixing with detrital silts and muds during deposition.

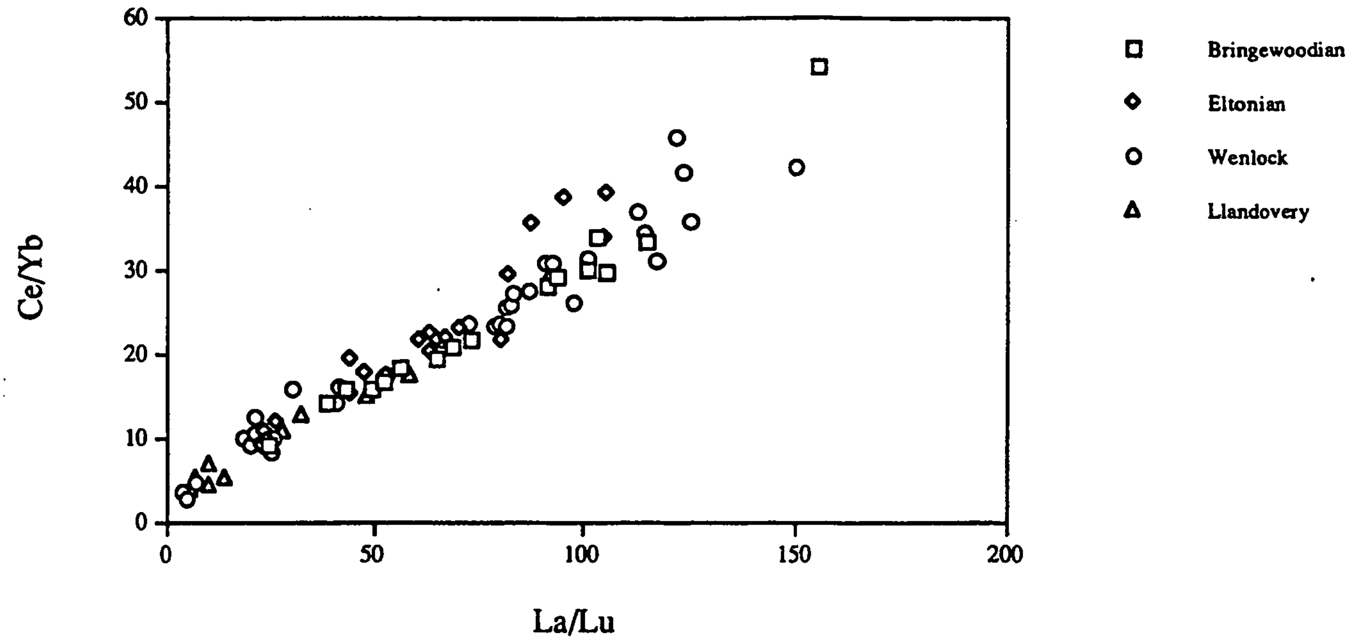

Figure 14 Ratios of light and heavy REE in K-bentonites show a range of LREE enrichment throughout the Silurian. In a very general way, the older Llandovery and early Wenlock samples show somewhat greater LREE enrichment than do the Ludlow samples. This may reflect variations in the source magmas throughout the interval, or perhaps variations in the amount of felsic crustal material contaminating upper mantle parental magmas.

Volcanic source

Based on comparison with other Paleozoic K-bentonites the relatively fine grain size of the residual primary phenocrysts of quartz, feldspar, biotite, apatite and zircon further indicate the source vents were located tens to hundreds of kilometers from the depositional sites (Zhang & Huff 1994). Although all original pumice and ash has devitrified, theoretical studies (Walker 1981) have shown that plinian and co-ignimbrite eruptions typically produce ejecta of which up to 50% of the total may be composed of ash and dust size particles. Ultraplinian eruptions may have degrees of fragmentation that produce of the order of 60-70% ejecta finer than 63 μm in diameter. Phenocryst size of primary particles should not be expected to differ greatly from original tephra size provided there has been no large-scale authigenesis of feldspars. Many of the lateral changes in the character of plinian fallout deposits are well established. With increasing distance from the vent there is a overall 1) decrease in thickness, 2) decrease in maximum grain size, 3) decrease in median grain size, and 4) increase in sorting (Walker 1981).

Bergström et al. (1992) noted the similarity in the vertical distribution pattern of British and Baltoscandian Silurian K-bentonite successions. The fact that both these successions contain a large number of beds and that very few such beds are known from this interval in eastern North America, in contrast to the Ordovician occurrences, suggests that the source area was closer to the British Isles and Baltoscandia than to North America. An exception is the occurrence of a sequence of Silurian K-bentonites in the Arisaig area in Nova Scotia, eastern Canada, where the lower member of the Ross Brook Formation contains at least 13 K-bentonites identified as tuffs by Boucot et al. (1974). It is possible that active subduction along the Laurentian margin during the Silurian closure of Iapetus produced a dominantly eastward transport of airborne ashes which were preserved in the siliciclastic and carbonate sequences of Baltica and Avalonia, but that some of the ash was transported westward to what is now Nova Scotia. Further investigations on both sides of Iapetus are needed to resolve both the event-stratigraphic significance of the K-bentonites as well as the precise location of their source volcanoes.

Discussion and conclusions

Trace and major element geochemical data indicate Llandovery through Ludlow K-bentonites in southern Great Britain were derived from siliceous, subalkaline magmas of largely dacite to rhyolite composition. These magmas were, for the most part, calc-alkaline in character and erupted in subduction-related, plate margin to ensialic margin settings.

Although there is no consensus on the precise timing and style of collision events associated with the closing of Iapetus and the joining of Eastern Avalonia, Baltica and Laurentia, the nature and distribution of Silurian K-bentonites provide strong evidence leading to two conclusions: 1) source volcanoes were plate margin, subduction-related, silicic vents, and 2) their explosivity continued unabated from earliest Llandovery through Ludlow with sufficient repetitiveness and energy to leave abundant stratigraphic records throughout northwestern Europe and parts of eastern North America. McKerrow et al. (1991) have provided one widely cited interpretation of the paleogeographic positions of these tectonic regimes during the Llandovery. Previous studies have concluded that Avalonia collided with Baltica in early Ashgill times but that deposition in the Southern Uplands trench continued well into the Silurian. But whether that collision was "hard" (Soper & Woodcock 1990) or "soft" (Pickering et al. 1988) is not resolved on the basis of K-bentonite chemistry. However, the nature and distribution of Silurian K-bentonites would tend to support a model of an open Iapetus through much of the Silurian with a significant turning point coinciding with the cessation of explosive volcanism during Ludlow time. Thirlwall (1988) has described a change in geochemical signature among calc-alkaline arc-related volcanics at 410 Ma which coincides approximately with the Ludlow-Pridoli boundary. The subsequent development of a series of plutonic intrusions, mainly during the early to mid-Devonian may not have been subduction-related but caused instead by a steepened thermal gradient associated with tectonic loading and foreland basin development. Finally, atmospheric circulation models proposed for the early and mid Silurian (Wilde et al. 1991) would account for a preponderance of airfall ash in northwestern Europe and a relative scarcity in North America if the source volcanoes were located to the northeast of Avalonia along the Iapetus margin. A similar source and distribution pattern was envisaged by Huff et al. (1993) for Ordovician K-bentonites in Great Britain, suggesting the explosive volcanism which accompanied tectonic closure and subduction along the margin of Iapetus through the lower Palaeozoic was active until at least late in the Silurian.

Acknowledgments

This work was supported by NSF grant INT-8419409 to WDH. We appreciate reviews of an earlier draft by Drs N. Fortey and R. Merriman.

References

Abdel-Rahman, A.-F.M. (1994) Nature of biotites from alkaline, calc-alkaline, and peraluminous magmas. *Journal of Petrology*, **35**, 525-541.

André, L., Hertogen, J. & Deutsch, S. (1986) Ordovician-Silurian magmatic provinces in Belgium and the Caledonian orogeny in middle Europe. *Geology*, **14**, 879-882.

Aronson, J.L. & Lee, M. (1986) K/Ar systematics of bentonite and shale in a contact metamorphic zone, Cerrillos, New Mexico. *Clays and Clay Minerals*, **34**, 483-487.

Bassett, M.G., Cocks, L.R.M., Holland, C.H., Rickards, R.B. & Warren, P.T. (1975) *The Type Wenlock Series.* Institute of Geological Sciences, Report **75/13**, 19 pp.

Batchelor, R.A. and Clarkson, E.N.K. (1993) Geochemistry of a Silurian metabentonite and associated apatite from the North Esk Inlier, Pentland Hills. *Scottish Journal of Geology*, **29**, 123-130.

Bergström, S.M. (1989) Use of graphic correlation for assessing event-stratigraphic significance and trans-Atlantic relationships of Ordovician K-bentonites. *Proceedings of the Estonian Academy of Sciences*, **38**, 55-59.

Bergström, S.M., Huff, W.D. & Kolata, D.R. (1992) Silurian K-bentonites in the Iapetus Region: A preliminary event-stratigraphic and tectonomagmatic assessment. *Geologiska Föreningens I Stockholm Förhandlingar*, **114**, 327-334.

Boucot, A.J., Dewey, J.F., Dineley, D., Fletcher, R., Fyson, W.K., Griffin, J.G., Hickox, C.F., McKerrow, W.S. & Ziegler, A.M. (1974) Geology of the Arisaig area, Antigonish County, Nova Scotia. *Geological Society of America Special Paper*, **139**, 1-191.

Cetin, K. & Huff, W.D. (1995) Characterization of untreated and alkylammonium ion exchanged illite/smectite by high resolution electron microscopy. *Clays and Clay Minerals*, **43**, 337-345.

Cummins, W.A. (1957) The Denbigh Grits; Wenlock greywackes in Wales. *Geological Magazine*, **94**, 433-451.

Davies, J.H., Holroyd, J., Lumley, R.G. & Owen-Roberts, D. (1978) *Geology of Powys in Outcrop.* Radnor Museum, Llandrindod Wells, Powys, 220pp.

Delano, J.W., Tice, S.J., Mitchell, C.E. & Goldman, D. (1994) Rhyolitic glass in Ordovician K-bentonites: A new stratigraphic tool. *Geology*, **22**, 115-118.

Dodge, F.C.W., Smith, V.C. & Mays, R.E. (1969) Biotites from granitic rocks of the central Sierra Nevada batholith, California. *Journal of Petrology*, **10**, 250-271.

Elliott, C.W. & Aronson, J.L. (1987) Alleghanian episode of K-bentonite illitization in the southern Appalachian Basin. *Geology*, **15**, 735-739.

Fetzer, J.A. (1973) *Biostratigraphic evaluation of some Middle Ordovician bentonite complexes in eastern North America.* Masters Thesis, The Ohio State University.

Foster, M.D. (1960) Interpretation of the composition of trioctahedral micas. *U.S. Professional Paper* **354-B**, 11-49.

Goldman, D., Mitchell, C.E., Bergström, S.M., Delano, J.W. & Tice, S. (1994) K-bentonites and graptolite biostratigraphy in the Middle Ordovician of New York State and Quebec: a new chronostratigraphic model. *Palaios*, **9**, 124-143.

Hagemann, F. (1966) Silurian bentonites of the Oslo region. *Norges Geologiske Undersökelse Årsbok 1965*, **242**, 44-61.

Harrison, W.B. (1991) Middle Silurian ash beds from the Michigan Basin. *Geological Society of America Abstracts with Programs*, **23**, A17.

Hay, R.L., Lee, M., Kolata, D.R., Matthews, J.C. & Morton, J.P. (1988) Episodic potassic diagenesis of Ordovician tuffs in the Mississippi Valley area. *Geology*, **16**, 743-747.

Haynes, J.T. (1989) *The mineralogy and stratigraphic setting of the Rocklandian (Upper Ordovician) Deicke and Millbrig K-bentonite beds along the Cincinnati arch and in the southern Valley and Ridge*. Ph.D. Thesis, University of Cincinnati.

Haynes, J.T. (1994) The Ordovician Deicke and Millbrig K-bentonite beds of the Cincinnati Arch and the southern Valley and Ridge Province. *Geological Society of America Special Paper*, **290**, 1-80.

Hildreth, W. (1977) *The magma chamber of the Bishop Tuff: Gradients in temperature, pressure, and composition*. Ph.D. Thesis, University of California, Berkeley.

Hildreth, W., Halliday, A.N. & Christiansen, R.L. (1991) Isotopic and chemical evidence concerning the genesis and contamination of basaltic and rhyolitic magma beneath the Yellow Plateau volcanic field. *Journal of Petrology*, **32**, 63-138.

Hower, J., Eslinger, E.V., Hower, M.E. & Perry, E.A. (1976) Mechanism of burial metamorphism of artillaceous sediment: 1. Mineralogical and chemical evidence. *Geological Society of America Bulletin*, **87**, 725-737.

Huff, W.D., Anderson, T.B., Rundle, C.C. & Odin, G.S. (1991) Chemostratigraphy, K-Ar ages and illitization of Silurian K-bentonites from the central belt of the Southern Uplands-Down-Longford terrane, British Isles. *Journal of the Geological Society, London*, **148**, 861-868.

Huff, W.D. & Kolata, D.R. (1989) Correlation of K-bentonite beds by chemical fingerprinting using multivariate statistics. Pp 567-577 in: *Quantitative Dynamic Stratigraphy*. (T.A. Cross, editor). Prentice-Hall, Englewood Cliffs, NJ.

Huff, W.D., Kolata, D.R. & Bergström, S.M. (1992) Eruption characteristics of the Middle Ordovician Deicke and Millbrig K-bentonites. *Geological Society of America Abstracts with Programs*, **24**, 199.

Huff, W.D., Merriman, R.J., Morgan, D.J. & Roberts, B. (1993) Distribution and tectonic setting of Ordovician K-bentonites in the United Kingdom. *Geological Magazine*, **130**, 93-100.

Huff, W.D. & Morgan, D.J., (1990) Stratigraphy, mineralogy and tectonic setting of Silurian K-bentonites in southern England and Wales: *Proceedings of the 9th International Clay Conference, Strasbourg, Vol. IV, 33-42 (Sciences Geologiques 88).*

Izett, G.A. (1981) Volcanic ash beds: Recorders of Upper Cenozoic silicic pyroclastic volcanism in the western United States. *Journal of Geophysical Research*, **86**, 10200-10222.

Jakes, P. and White, A.J.R. (1972) Major and trace element abundances in volcanic rocks of orogenic areas. *Geological Society of America Bulletin*, **83**, 29-40.

Johnson, M.E. (1981) Correlation of Lower Silurian strata from the Michigan Upper Peninsula to Manitoulin Island. *Canadian Journal of Earth Sciences*, **18**, 869-883.

Jürgenson, E. (1964) Silurian metabentonites of the Estonian S.S.R. Pp. 87-89 in: *Litologiya paleozoyskikh otlozhenug Estonii*. Eesti NSV

Teaduste Akadeemia Toimentised Geoloogia Instituut, Tallinn.

Kolata, D.R., Frost, J.K. & Huff, W.D. (1987) Chemical correlation of K-bentonites in the Middle Ordovician Decorah Subgroup, upper Mississippi Valley. *Geology*, **15**, 208-211.

Lagaly, G. (1982) Layer charge heterogeneity in vermiculites. *Clays and Clay Minerals*, **30**, 215-222.

Lagaly, G., and Weiss, A. (1976) The layer charge of smectitic layer silicates. *Proceedings of the International Clay Conference, Mexico City, Mexico, 1975*, 157-172.

McKerrow, W.S., Dewey, J.F. & Scotese, C.R. (1991) The Ordovician and Silurian development of the Iapetus Ocean. *Special Papers in Palaeontology*, **44**, 165-178.

Merriman, R.J. & Roberts, B. (1990) Metabentonites in the Moffat Shale Group, Southern Uplands of Scotland: Geochemical evidence of ensialic marginal basin volcanism. *Geological Magazine*, **127**, 259-271.

Moore, G.T., Jacobson, S.R., Ross, C.R., and Hayashida, D.N. (1994) A paleoclimate simulation of the Wenlockian (Late Early Silurian) world using a general circulation model with implications for early land plant paleoecology: *Palaeogeography, Palaeoclimatology, Palaeoecology*, **110**, 115-144.

Morgan, D.J. (1974) *Calcium montmorillonite and related mixed-layer illite-montmorillonite clays from the UK: The interdependence of physical properties with mineralogy, chemistry and mode of occurrence*. Ph.D. Thesis, University of London, 247pp.

Morgan, D.J. (1978) The K-bentonites at Woodbury quarry. Pp. 13-16 in: *Guidebook to Midlands of England, Itinerary E5*, Sixth International Clay Conference. Oxford.

Neilson, M.J. & Haynes, S.J. (1973) Biotites in calc-alkaline intrusive rocks. *Mineralogical Magazine*, **39**, 11-49.

Nusbaum, R.L., Thayer, P.A. & Harris, W.B. (1988) Source constraints based on biotite analyses for the 47 Ma Castle Hayne bentonite, North Carolina. *Southeastern Geology*, **29**, 29-39.

Odin, G.S., Baadsgaard, H., Bonhomme, M.G., Hunziker, J.C., Jeppsson, L., Spjeldnaes, N. & Zelvelder, M. (1986) Recherche de points de calibration Siluriens pour l'échelle numérique, approache multiméthode. *Terra Cognita*, **6**, 141.

Odin, G.S., Hurford, A.J., Morgan, D.J. & Toghill, P. (1986) K-Ar biotite date for Ludlovian bentonites from Great Britain. *Chemical Geology (Isotope Geoscience Section)* **59**, 127-131.

Pearce, J.A., Harris, N.B.W. & Tindle, A.G. (1984) Trace element discrimination diagrams for the tectonic interpretation of granitic rocks. *Journal of Petrology*, **25**, 956-983.

Pickering, K.T., Bassett, M.G. & Siveter, D.J. (1988) Late Ordovician-Early Silurian destruction of the Iapetus Ocean: Newfoundland, British Isles and Scandinavia. *Transactions of the Royal Society of Edinburgh: Earth Sciences*, **79**, 361-382.

Reynolds, R.C. (1980) Interstratified clay minerals. Pp. 249-303 in: *Crystal Structures of Clay Minerals and their X-ray Identification* (G.W. Brindley and G. Brown, editors). Mineralogical Society, London.

Reynolds, R.C., Jr., (1985) *NEWMOD: A computer program for the calculation of one-dimensional diffraction patterns of mixed-layer clays*. R.C. Reynolds, 8 Brook Rd., Hanover, NH.

Roberts, B. & Merriman, R.J. (1990) Cambrian and Ordovician metabentonites and their relevance to the origins of associated mudrocks in the northern sector of the Lower Palaeozoic Welsh marginal basin. *Geological Magazine*, **127**, 31-43.

Roberts, M.P. & Clemens, J.D. (1993) Origin of high-potassium, calc-alkaline, I-type granitoids. *Geology*, **21**, 825-828.

Romano, M. & Spears, D.A. (1991) Bentonites from the Horton Formation (Upper Silurian) of Ribblesdale, Yorkshire. *Proceedings of the Yorkshire Geological Society*, **48**, 277-285.

Ross, R.J., Jr., et al. (1982) Fission-track dating of British Ordovician and Silurian stratotypes. *Geological Magazine*, **119**, 135-153.

Samson, S.D., Patchett, P.J., Roddick, J.C. & Parrish, R.R. (1989) Origin and tectonic setting of Ordovician bentonites in North America: Isotopic and age constraints. *Geological Society of America Bulletin*, **101**, 1175-1181.

Snäll, S. (1978) Silurian and Ordovician bentonites of Gotland (Sweden). *Stockholm Contributions in Geology*, **31**, 1-80.

Soper, N.J. & Woodcock, N.H. 1990. Silurian collision and sediment dispersal patterns in southern Britain. *Geological Magazine*, **127**, 527-542.

Środon, J., Morgan, D.J., Eslinger, E.V., Eberl, D.D., and Karlinger, M.R. (1986) Chemistry of illite/smectite and end-member illite. *Clays and Clay Minerals*, **34**, 368-378.

Steiger, R.H. & Jager, E. (1977) Subcommission on geochronology: Convention on the use of decay constants in geo- and cosmochronology. *Earth and Planetary Science Letters*, **36**, 359-362,

Stose, G.W. & Jonas, A.I. (1927) Ordovician shale and associated lava in southeastern Pennsylvania. *Geological Society of America Bulletin*, **38**, 505-536.

Sun, H. and Huff, W.D. (1995) Tectonomagmatic setting of the Osmundsberg K-bentonite (Lower Silurian) in northwestern Europe. *International Union of Geodesy and Geophysics Abstracts Volume*, XXI General Assembly, Boulder, v. Week A, p. A439.

Teale, C.T. & Spears, D.A. (1986) The mineralogy and origin of some Silurian bentonites, Welsh Borderland, U.K. *Sedimentology*, **33**, 757-765.

Thirlwall, M.F. (1988) Wenlock to mid-Devonian volcanism of the Caledonian-Appalachian orogen. Pp. 415-426 in: *The Caledonian-Appalachian Orogen*. (A.L. Harris and D.J. Fettes, editors). Geological Society of London, 415-426.

Trewin, N.H. (1971) Potassium bentonites in the Wenlock Limestone of Shropshire. *Mercian Geologist*, **4**, 1-7.

Tucker, R.D., Krogh, T.E., Ross, R.J., Jr. & Williams, S.H. (1990) Time-scale calibration by high-precision U-Pb zircon dating of interstratified volcanic ashes in the Ordovician and Lower Silurian stratotypes of Britain. *Earth and Planetary Science Letters*, **100**, 51-58.

Walker, G.P.L. (1981) Plinian eruptions and their products. *Bulletin of Volcanology*, **44**, 223-240.

Watkins, R. (1979) Benthic community organization in the Ludlow Series of the Welsh Borderland: *Bulletin of the British Museum of Natural History*, **31**, 175-280.

White, D.E. & Lawson, J.D. (1978) *The stratigraphy of new sections in the Ludlow Series of the type area, Ludlow, Salop, England*. Institute of Geological Sciences, Report **78/30**, 10 pp.

Whitney, J.A. & Stormer, J.C., Jr. (1985) Mineralogy, petrology, and magmatic conditions from the Fish Canyon Tuff, Central San Juan Volcanic Field, Colorado. *Journal of Petrology*, **26**, 726-762.

Wilde, P., Berry, W.B.N. & Quinby-Hunt, M.S., (1991) Silurian oceanic and atmospheric circulation and chemistry. Pp. 123-143 in: *The Murchison Symposium: Proceedings of an International Conference on the Silurian System, Keele*. Special Papers in Palaeontology.

Winchester, J.A. & Floyd, P.A. (1977) Geochemical discrimination of different magma series and their differentiation products using immobile elements. *Chemical Geology*, **20**, 325-343.

Zhang, Y.-S. & Huff, W.D. (1994) Grain size characteristics of a Middle Ordovician eruption and its source area: *Abstracts of the Eighth International Conference on Geochronology, Cosmochronology and Isotope Geology*, 364 U.S. Geological Survey, Berkeley.

Appendix A - Locality register

Sample	Location
SI-1	Eltonian Beds in stream section at Upper Millichope (SO 5202 8955).
SI-2	Same as SI-1.
SI-3	Same as SI-1.
SI-6	Late Llandovery purple shales along the Onny River 1 m above unconformable contact with the Caradoc Acton Scott Formation (SO 4262 8532).
SI-7	Upper Brigewoodian Beds, Mortimer Forest near Ludlow (SO 4956 7250) (= bed C4 of White & Lawson, 1978).
SI-8	Same as SI-7 (= bed C2 of White & Lawson, 1978).
SI-9	Same as SI-7 (= bed C12 of White & Lawson, 1978).
SI-10	Eltonian Beds, Mortimer Forest near Ludlow (SO 4750 7187) (= bed A4/A5 of White and Lawson, 1978).
SI-11	Same as SI-10 (= bed A5 of White and Lawson, 1978).
SI-12 to SI-14	Bringewoodian Beds, Woodbury Quarry near Abberley (SO 7404 6354).
SI-15 to SI-42	Same as SI-12 to SI-14.
SI-43 to SI-46, 50, & 51	Upper Bringewoodian Beds, Perton Quarry, Woolhope Inlier (SO 5945 3983).
SI-47 to SI-49	Much Wenlock Formation, Woolhope Inlier (SO 5718 3690).
SI-52 & SI-53	Early Wenlock, Haugh Wood section, Woolhope Inlier (SO 5875 3781).
SI-55 to SI-58	Woolhope Quarry, Woolhope Inlier (SO 6125 3580).
SI-59 to SI-61	Overbury Quarry, Woolhope Inlier (SO 6111 3642).
SI-62	Scutterdine Quarry, Woolhope Inlier (SO 5775 3691).
SI-63 to SI-65	Upper Bringewoodian Beds, Sleaves Oak Quarry, Woolhope Inlier (SO 6295 3450).
WDH-1 to WDH-4	Wenlock Limestone, Coates Quarry (SO 604 994) (ref. Trewin, 1971).
WDH-5 to WDH-8	Coalbrookdale Formation, Eaton (SO 5020 8999) (ref. Ross et al., 1982).
WDH-12	Eltonian Beds near Penybont (SO 1556 5965) (ref. Davies et al., 1978, Loc. #50).
WDH-21 & WDH-22	Wenlock Beds near Builth Wells (SN 983 531) (ref. Davies et al., 1978, Loc. #59).
WDH-25	Upper Ludlow Beds near Newton along the A483 (SO 0913 8462) (ref. Davies et al., 1978, Loc. #26).
WDH-26 to WDH-33	Llandovery Purple Shales, Brickworks yard at Buttington (SJ 265 100) (ref. Davies et al., 1978, Loc. #14).
WDH 47	Llandovery shales, stream section, Etsell, Shropshire (SJ 349 029)
WH-34	Wenlock sandstones, Tan-Y-Fael Quarry (SJ 014 015).
696E	Wenlock Limestone, BGS Borehole No. 1, Manor Farm, Rushall, Staffordshire (SK 035 009).
786A	Wenlock Limestone, Gleedon Hill Quarry, Ironbridge, Shropshire (SJ 633 017).
B1	Upper Bringewood Beds (Ludlow), Llangibi Castle, Monmouth (ST 3655 9777).
B2	Same locality as B1, 1 m below.
B6	Wenlock Limestone, Penny Hill Quarry, Marcle, Worcester (SO 751 616).
B7	Same locality as B6, 2 m below.
B8	Aymestry Limestone, Shavers End Quarry, Abberley, Worcester (SO 771 680).
B9	Wenlock Limestone, Wallhouse Plantation Quarry, Shelsley Beauchamp, Worcester (SO 751 637).
B13	Sleaves Oak Beds (Ludlow), Deans Place Quarry, Much Marcle, Hereford (SO 6365 3150).
GSO-B15	Wenlock Limestone, Leasowes Farm, Shropshire.

GSO-B2	Same locality as GSO-B15, near Wenlock/Llandovery boundary.	LHF-3036 to LHF-6894	Wenlock Beds in the Lower Hill Farm Borehole (SO 5817 9788) (ref. Bassett et al., 1975).
A2 to A22	Eltonian Beds (Ludlow), Mortimer Forest near Ludlow (ref. White & Lawson, 1978).		